

# Spatial Modelling of Cellular Networks

Mengjie Zhao  
U5418761

Supervised by Dr. Xiangyun (Sean) Zhou

June 2015



A thesis submitted in part fulfilment of the degree of  
Bachelor of Engineering  
The Department of Engineering  
Australian National University

This thesis contains no material which has been accepted for the award of any other degree or diploma in any university. To the best of the author's knowledge, it contains no material previously published or written by another person, except where due reference is made in the text.

Mengjie Zhao  
1 June 2015

©Mengjie Zhao

---

# Acknowledgements

---

First and foremost, I would like to offer my thanks to Dr. Xiangyun (Sean) Zhou, for providing me with the opportunity to undertake this research project, by finishing which I obtained more insight knowledge of the cellular networks. The constant guidance and advice help me overcoming the encountered issues, and I really appreciate the time and patience on mentoring me. Thank you very much.

Thank you to my friend Yizhou, for always driving me home at midnight when I miss the last turn of the Unisafe bus. Thank you to Yanning, Mengzhuo and all my BIT mates, it is you that makes the oversea life feel like home to me. Thank you to Johnny Xu for pushing me to finish the GRE test, that period of time will inspire me forever.

Finally, I would like to thank my dad and mom, for the consistent support and understanding.

---

# Abstract

---

Grid models are widely applied in studying and researching the cellular networks. However, compared with the real world cellular network deployment, the grid models are highly ideal. Researchers proposed a random deployment model, within in which the base station locations of the cellular network are determined by Poisson point process. In this thesis, evaluations of coverage probability and average achievable rate performance of the newly proposed random deployment model and the traditional grid models are carried out. In doing this, firstly the cellular network models are constructed. After that, according to the constructed models, the coverage probability and the average achievable rate of each cellular network model is evaluated respectively, in both downlink access scenario and uplink access scenario. It is discovered that the random deployment model always provides conservative but accurate coverage probability and average achievable rate performance. Additionally, due to the mathematical attractable property, it is concluded that the random deployment model is a useful tool which can be utilized to study and research cellular networks.

---

# Contents

---

<b>Acknowledgements</b>	<b>i</b>
<b>Abstract</b>	<b>ii</b>
<b>List of Figures</b>	<b>vi</b>
<b>List of Tables</b>	<b>vii</b>
<b>List of Tables</b>	<b>vii</b>
<b>List of Abbreviations</b>	<b>viii</b>
<b>1 Introduction</b>	<b>1</b>
1.1 Cellular Network Basics . . . . .	1
1.2 Problem Statement and Project Aims . . . . .	3
1.3 Previous Works . . . . .	5
1.4 Thesis Organisation . . . . .	6
<b>2 Simulation Model Construction</b>	<b>7</b>
2.1 Simulation Tool . . . . .	7
2.2 Deployment Methodologies . . . . .	7
2.3 Wireless Channel Model . . . . .	9
2.3.1 Path Loss Effect . . . . .	9
2.3.2 Fading Channel . . . . .	10
2.3.3 Additive White Gaussian Noise . . . . .	11
2.4 Fractional Power Control . . . . .	11
2.5 Default Network Settings . . . . .	13
2.6 Summary . . . . .	13
<b>3 Coverage Probability Analysis</b>	<b>14</b>
3.1 Coverage Probability Definition . . . . .	14
3.2 Downlink Access Analysis . . . . .	15
3.2.1 Network Models with Default Settings . . . . .	16
3.2.2 Network Models with Various Path Loss Factor . . . . .	18
3.2.3 Network Models with Various AWGN Power . . . . .	20

3.2.4	Network Models with Various Base Station Density . . . . .	21
3.3	Uplink Access Analysis . . . . .	23
3.3.1	Network Models with Default Settings . . . . .	25
3.3.2	Network Models with Various Path Loss Factor . . . . .	26
3.3.3	Effects of Changing Power Control Factor . . . . .	27
3.4	Border Effect . . . . .	30
3.5	Summary . . . . .	30
<b>4</b>	<b>Average Achievable Rate Analysis</b>	<b>32</b>
4.1	Ergodic Rate and Parameter $K$ . . . . .	32
4.1.1	Ergodic Rate . . . . .	32
4.1.2	Parameter $K$ . . . . .	33
4.2	Downlink Access Analysis . . . . .	35
4.2.1	Network with Default Settings . . . . .	35
4.2.2	Network with Various Path Loss Factor . . . . .	39
4.3	Uplink Access Analysis . . . . .	40
4.3.1	Network with Default Settings . . . . .	41
4.3.2	Network with Various Path Loss . . . . .	42
4.3.3	Network with Various Power Control . . . . .	43
4.4	The Combined Access Scenario . . . . .	44
4.5	Summary . . . . .	46
<b>5</b>	<b>Conclusion and Future Works</b>	<b>47</b>
5.1	Conclusion . . . . .	47
5.2	Future Works . . . . .	48
<b>Bibliography</b>		<b>49</b>
<b>A</b>	<b>MATLAB Scripts</b>	<b>52</b>
A.1	MATLAB scripts of coverage probability . . . . .	52
A.2	MATLAB scripts of average achievable rate . . . . .	71

---

# List of Figures

---

1.1	A typical cellular network system . . . . .	1
1.2	Diamond grid model . . . . .	3
1.3	Hexagonal grid model . . . . .	3
1.4	An urban area BS deployment . . . . .	4
1.5	Random BS deployment . . . . .	4
2.1	Uplink fractional power control model . . . . .	12
3.1	Default PPP model . . . . .	16
3.2	Default hexagonal model . . . . .	16
3.3	Default diamond model . . . . .	16
3.4	Default coverage probabilities . . . . .	16
3.5	Path loss factor is 2.5 . . . . .	19
3.6	Path loss factor is 4.5 . . . . .	19
3.7	Path loss factor is 5.5 . . . . .	19
3.8	Path loss factor is 6 . . . . .	19
3.9	$P_n = -100\text{dBm}$ and $-170\text{dBm}$ . . . . .	21
3.10	$P_n = -100\text{dBm}$ and $-80\text{dBm}$ . . . . .	21
3.11	16 and 36 base stations . . . . .	22
3.12	64 and 36 base stations . . . . .	22
3.13	Uplink PPP model . . . . .	24
3.14	Uplink diamond model . . . . .	24
3.15	Uplink hexagonal model . . . . .	24
3.16	Uplink coverage probability . . . . .	24
3.17	Path loss factor is 2.5 . . . . .	26
3.18	Path loss factor is 4.5 . . . . .	26
3.19	Path loss factor is 5.5 . . . . .	26
3.20	Path loss factor is 6 . . . . .	26
3.21	PPP model with PCFs . . . . .	28
3.22	Diamond model with PCFs . . . . .	28
3.23	Hexagonal model with PCFs . . . . .	28
3.24	Uplink coverage PCF=0.4 . . . . .	28
4.1	Rate of default models (No K) . . . . .	35

4.2	Rate of default models . . . . .	35
4.3	Path Loss Factor is 3.5 . . . . .	39
4.4	Path Loss Factor is 4.5 . . . . .	39
4.5	Default Uplink Rate (No K) . . . . .	41
4.6	Default Uplink Rate . . . . .	41
4.7	Path Loss Factor is 3.5 . . . . .	43
4.8	Path Loss Factor is 4.5 . . . . .	43
4.9	Power control factor is 1 . . . . .	44
4.10	Power control factor is 0.8 . . . . .	44
4.11	Power control factor is 0.6 . . . . .	44
4.12	Power control factor is 0.4 . . . . .	44
4.13	Rate of diamond grid model . . . . .	45
4.14	Rate of PPP model . . . . .	45

---

# List of Tables

---

2.1	Default cellular network settings . . . . .	13
4.1	Rate comparison when $P_t/P_n = 90dB$ . . . . .	37
4.2	Rate comparison when $P_t/P_n = 110dB$ . . . . .	37
4.3	Rate comparison when $P_t/P_n = 90dB$ . . . . .	42
4.4	Rate comparison when $P_t/P_n = 110dB$ . . . . .	42

---

# List of Abbreviations

---

AWGN	Additive white Gaussian noise	DSSS
BSC	Base station controller	
CDMA	Code division multiple access	
DS-CDMA	Direct-sequence code division multiple access	
	Direct-sequence spread spectrum	
FFR	Fractional frequency reuse	
GSM	Global System for Mobile Communications	
MSC	Mobile switching centre	
OFDM	Orthogonal frequency-division multiplexing	
PHCP	Poisson hard-core process	
PPP	Poisson point process	
PSTN	Public switched telephone network	
RRM	Radio resource management	
SINR	Signal-to-interference-plus-noise ratio	
SNR	Signal-to-noise ratio	
TDMA	Time division multiple access	

---

# Introduction

---

This chapter aims to provide an introduction to the thesis. Section 1.1 presents a brief overview of cellular networks. The issues to be investigated and the motivation of carrying out the research is included in Section 1.2. Some previous works are presented in Section 1.3 and the thesis organisation is demonstrated in Section 1.4.

## 1.1 Cellular Network Basics

Starting from 1980s, cellular networks have kept developing for nearly 40 years, bringing a wide range of applications and convenience to human. A cellular system normally consists of base stations, mobile terminals and other supportive infrastructure. More specifically, in a cellular network, a land area such as a city is subdivided into regular and none overlapping cells, which could be diamond or hexagonal. Each cell contains one base station, serving numerous mobile terminals resided in the same cell. When a mobile user moves from one cell to another cell, a handoff would occur, i.e., the serving base station changes. It requires additional signaling and processing [1]. A simplified cellular network system is showed in Figure 1.1[2]:

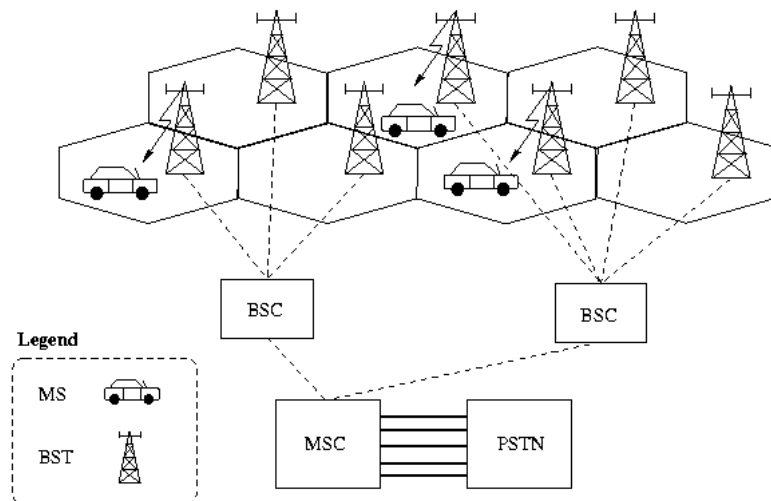


Figure 1.1: A typical cellular network system

It can be observed that each base station is serving mobile terminals who resided in the cell. Base stations are controlled by the Base Station Controller (BSC), and BSCs in the area are connected to the Mobile Switching Center (MSC), which can communicate with the Public Switched Telephone Network (PSTN).

Cellular systems are a type of infrastructure-based network that makes efficient use of spectrum by reusing it at spatially separated locations [3]. Within a cellular network, the entire frequency spectrum is split into channels and each cell is assigned with a subset of channels. As a result, in the whole network, frequency spectrum is reused. There will be no interferences between adjacent cells since they use different sets of channels. The distance between cells using the same channels (co-channel cells) is enlarged due to the spatial trait of cellular networks, hence the interferences are largely reduced and the network has a relatively good performance.

As introduced above, reusing the frequency spectrum of a cellular network is the core technique applied to increase the number of mobile users that can be supported by the cellular network, as a result, it can be confirmed that reusing the entire frequency spectrum in every cell will maximize the total number of mobile users that can be supported by the whole cellular network, given that the interference between cells is carefully managed. However, this aggressive spectrum reuse is hard to achieve because managing the interference for a particular cell is involved, since interferences come from all other cells within in this cellular network. Fortunately, some advanced interference management techniques have been proposed and applied, hence the aggressive spectrum reuse has been achieved. For example, the direct sequence spread spectrum (DSSS) technique is applied in the direct sequence code division multiple access (DS-CDMA) network to reduce the interference between one mobile user and base stations located in other cells. In addition, as 4G cellular networks standards also target in this aggressive spectrum reuse, therefore some other advance techniques such as semi-static radio resource management (RRM) through adaptive fractional frequency reuse (FFR) mechanisms and power control are also applied to better manage the interference [4].

Within a cellular network, mobile users may communicate with their nearest base stations in two basic methodologies, namely downlink access and uplink access. In a downlink access scenario, the nearest base station transmits data to the same cell mobile users through the wireless channel and other co-channel base stations act as interference sources. Conversely, in an uplink access scenario, a mobile user sends data to its nearest base station through the wireless channel and other users applying the same channels act as interference sources. Apparently users can also

perform these two access methodologies simultaneously, and this will involve more advanced signal processings.

The techniques applied in cellular networks keep evolving, providing better service to mobile users. Code division multiple access (CDMA) is a popular technique applied in 3G networks, which can provide fast data transmission between mobile users and base stations. Recently, orthogonal frequency division multiplexing (OFDM) is implemented in the LTE network, offering even faster data transmission and making mobile online gaming and video calls become possible. Overall, cellular networks significantly improve human's life quality and provide much convenience. Implementing researches on the cellular network would benefit humanity a lot.

## 1.2 Problem Statement and Project Aims

With the development of smartphone technologies, mobile users consume an increasing amount of data by using their smartphones and this trend would not stop in future years [5]. Cellular networks now are under ever-increasing pressure to increase the volume of data they can deliver to consumers [6]. Consequently, more insight researches and understandings of cellular networks are necessary. In past years, the analytical model that researchers frequently used is the grid model – the cell shape is regular, like diamond or hexagonal as showed in Figure 1.2 and Figure 1.3 respectively. Base stations (red dots) are placed at the centre of the cell while mobile terminals are randomly scattered in the network area. This model is intuitive but over ideal, since most real world cells do not have regular shape. In addition, the grid model is not very tractable because some analytical results are not close-formed, which means that complex computer simulations have to be implemented.

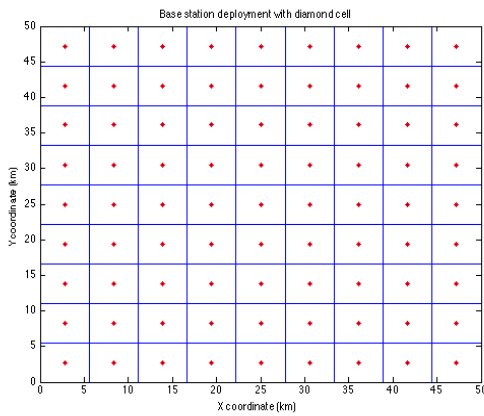


Figure 1.2: Diamond grid model

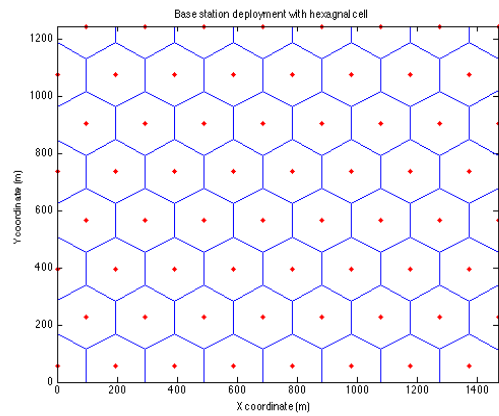


Figure 1.3: Hexagonal grid model

Under this circumstance, researchers proposed a new cellular network model, within which the base stations are scattered in the entire network area according to a homogeneous Poisson point process of density  $\lambda$ , as showed in Figure 1.5. Within this new network model, base stations have entirely and randomly generated coordinates, which are converse to the pre-determined base station coordinates in grid models. One real-world base station deployment of an urban area is showed in Figure 1.4 [7]. It can be observed that compared with grid models, the random deployment model can better simulate real-world base station deployment. However, it should be noticed that since the base stations coordinates are randomly generated, as a result, base stations will in some case closely locate together but still have a significant coverage area [6], as circled in Figure 1.5. Although this phenomenon rarely happens in real-world base station deployment, but compared with grid models, the random deployment model is already much better in simulating the base station deployment of the real world cellular network.

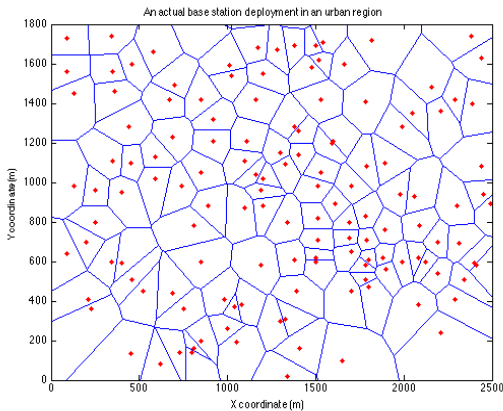


Figure 1.4: An urban area BS deployment

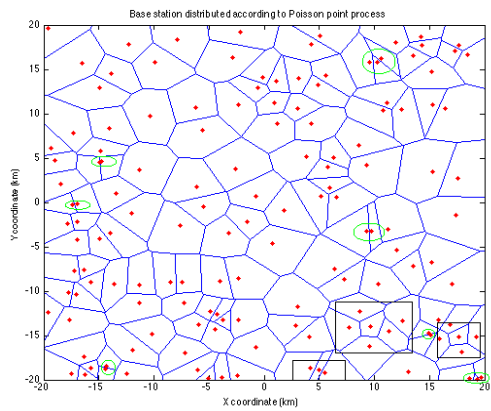


Figure 1.5: Random BS deployment

Many research works relating to this new model have been carried out and some initial but important results have been proposed. For instance, researchers illustrated that the random deployment model gives lower bound of cellular network performance such as downlink coverage and rate [6]. Also, compared with traditional grid models, the analytical results of the random deployment model are more tractable, sometimes can be simplified to simple integrals [6][8]. Within this context, this thesis aims to firstly introduce detailed information about the random deployment model then investigate the performance discrepancies between grid models and the random deployment model. In addition, testing and evaluation of existing proposed research results will be included and the thesis will also contain simulating and analyzing of some new network scenarios, such as more complex user behaviors that have not yet been touched by other researchers.

### 1.3 Previous Works

The idea of utilizing randomly distributed base stations to model real world base station deployment was initially proposed in 1997. Baccelli and other researchers proposed a new approach based on stochastic geometry to model telecommunication network architectures for purposes of strategic planning and economic analysis in [9]. Within this work, the preliminary architectures of the random deployment model were introduced and analysed. However, key network performances like coverage probability and network capacity, as well as the performance differences between grid models and the random deployment model were not clearly determined.

It was in 2011 that key performances analysis of the random deployment model was presented by Andrews and other researchers in [6]. Within this work, the general mathematical expressions of downlink coverage probability and network rate in a random deployment cellular network are derived. More importantly, under normal assumptions, the derived expressions can be simplified into very simple integrals, showing that the random deployment model is more tractable because exhaust computer simulations may not be necessary anymore.

Researchers also started to study the uplink transmissions in the random deployment model. Simple but rigorous uplink transmission models of the random deployment cellular networks were proposed in [10][11], illustrating that the random deployment model in the uplink access scenario shares same performance trend with that in the downlink scenario. Besides, by utilizing the random deployment model, researchers also proposed new mathematical frameworks for calculating the average error probability, outage probability and the handover probability of downlink cellular networks under certain modulation schemes [12][13]. Recently, Ge and other researchers investigated the spatial spectrum and energy efficiency of random cellular networks by integrating a Markov chain in the user access model, providing more insight understands of cellular network energy efficiency [14]. Overall, many researchers have started analysing the random deployment model and numerous valuable and helpful existing research results could provide suggestions and hints to solve the author's encountered issues.

## 1.4 Thesis Organisation

This thesis contains testing and evaluating current research results and testing network performances under new mobile user behaviors. Chapter 1 has demonstrated some basic knowledge relating to the cellular networks. It also demonstrates that carrying out researches on the random deployment model is necessary because this model is more mathematically tractable, compared with traditional grid cellular network models. Chapter 2 provides readers with detailed information and simulation methodologies of the constructed MATLAB models, which is consistently applied in the entire research project.

Chapter 3 serves to present cellular network coverage probability analysis in detail. Both uplink access and downlink access scenarios are studied and comparisons are carried out to better demonstrate the discrepancies in coverage probability performance between a random deployment model and grid models. Similar to Chapter 3, Chapter 4 displays the cellular network average achievable rate performance differences between a random deployment model and grid models. Again, both uplink access and downlink access scenarios are analysed and research results are clearly demonstrated. In addition, a combined user access scenario is included, to better simulate the real world user behaviors. Each chapter from Chapter 2 to Chapter 4 contains a summary section, concluding major contents in each chapter and finally, the thesis conclusions are derived in Chapter 5 and some suggestions for future works that could improve the research project are proposed.

# Simulation Model Construction

---

This chapter is intended to demonstrate the constructed MATLAB simulation models in detail. The simulation methodologies, cellular network parameters that consistently applied in all simulation models, as well as some essential assumptions are illustrated. This chapter helps readers understand the basic simulation models, as a result, further complex models applied in the following sections could be easily accepted, since they come from the basic models but containing more complex parameters or applying even advanced simulation methodologies.

Section 2.1 introduces the tool that is utilized to construct the simulation models. Section 2.2 provides specific information relating to the base station deployment and user deployment of simulative cellular network models. Wireless channel model applied in simulations is presented in Section 2.3. Section 2.4 is dedicated to introducing the fractional power control, which is a universal technique applied in mobile users' uplink access model of cellular networks. Finally, a set of default cellular network parameters and settings is displayed.

## 2.1 Simulation Tool

MATLAB R2012b is the software applied to carry out the cellular network model constructions and performance evaluations, due to its strong ability to process matrices, built-in functions and packaged toolboxes.

## 2.2 Deployment Methodologies

As discussed in Chapter 1, a cellular network covers a land area, which is going to be divided into regular or random shaped cells. Each cell contains one base station and numerous mobile users scattered in the whole land area. For consistency, within in this thesis, all cellular network models are presumed to be constructed on a  $10^6\ m^2$  land area.

Three different base station deployment models have been displayed in Figure 1.2, Figure 1.3 and Figure 1.5 respectively. The locations of base stations in a grid model are unchangeable, since they are determined to reside in the centre of a regular shaped cell. On the contrast, base station locations in a random deployment model are not pre-determined, but generated from a point process. A point process is a random collection of points that reside in same place [15]. Currently, the most popular point process applied to generate base station locations in a random deployment model is the homogenous Poisson point process (PPP). The validation of applying the PPP to determine base station locations is illustrated in [16]. In addition, researchers also carried out evaluations of other point process, such as Poisson hard-core process (PHCP) [17], under the context of cellular networks.

Evaluating different point processes is outside of the thesis scope. Consequently, in all simulation models, the homogenous PPP is applied to generate base station locations in a random deployment model and mobile user locations in both grid models and the random deployment model. The density of points in a land area can be calculated as the number of points divided by the area of the land. Therefore, mobile user density and base station density in a  $10^6 \text{ m}^2$  area can be defined by the following formulas:

$$\lambda_{US} = \frac{\text{Number of users}}{\text{Area}} = \frac{\text{Number of users}}{10^6} \quad (2.1)$$

$$\lambda_{BS} = \frac{\text{Number of base stations}}{\text{Area}} = \frac{\text{Number of base stations}}{10^6} \quad (2.2)$$

The default number of base stations and mobile users in a simulation model is 36 and 1000 respectively. Then the corresponding base station density and mobile user density can be accordingly calculated.

Theoretically the base station locations and user locations are generated from Poisson process, however, according to M. Pinsky and S. Karlin, conditioned on a fixed total number of events in an interval, the locations of those events are uniformly distributed in a certain way [18], also, PPP converges to uniform distribution on a infinite plane. As a result, base stations and users are assumed to uniformly distributed in the proposed land area in MATLAB models, and can be generated by using the MATLAB function `rand()`.

## 2.3 Wireless Channel Model

Compared with the traditional digital communication channel, the wireless communication channel is more complex due to its open-access and time-variant properties. This section focuses on demonstrating the assumptions and properties of the wireless communication channel implemented in the simulation models, since they significantly affect the cellular network performance. Within this section, firstly, large scale path loss effect and some essential parameters will be introduced. Then the fading channel properties and the noise characteristics will be illustrated. For simplicity, log-normal shadowing effect is not going to be taken into consideration, however, in future extension works, this effect could be enclosed to better simulate real world wireless communication channel model.

### 2.3.1 Path Loss Effect

In a cellular network, data or information is transmitted via radio waves between base stations and mobile users. Apparently base stations have to spend a large amount of energy on transmitting radio waves. The energy of received radio waves should be smaller than the original one due to the long travelled distance. This energy dissipation can be represented by the path loss effect. Path loss effect is caused by the dissipation of the power radiated by the transmitter as well as by effects of the propagation channel [3]. The power of the received signals for a particular mobile user can be calculated as follows:

$$P_r = \frac{P_t G_t G_r \lambda_c^2}{(4\pi)^2 (d)^\alpha} \quad (2.3)$$

Within this equation,  $P_r$  represents the power of received signals for a particular mobile user while  $P_t$  stands for the transmitted signal power from a base station.  $G_t$  and  $G_r$  represents transmitter antenna gain and receiver antenna gain respectively, which is determined by cellular network settings.  $\lambda_c$  stands for the radio wave carrier wavelength.  $d$  represents the distance between the chosen user and base station while  $\alpha$  is defined as the path loss exponent or path loss factor, which is the exponent of the distance  $d$ . Normally  $\alpha$  is determined by the cellular network environment, and it has significant influences on network performance, hence will be treated as a variable in future analysis. For consistency, the transmit power  $P_t$  is considered as 1 *Watt* in the following chapters of the thesis.  $\lambda_c$ ,  $G_t$  and  $G_r$  are treated as a constant since it is usually determined by cellular network settings and mobile carriers such as Vodafone and Telstra. Path loss effect is a major effect of wireless channels and will be taken into consideration in all simulation models.

### 2.3.2 Fading Channel

Small scale fading is another important wireless channel character that significantly impacts the cellular network performance. As discussed in Section 2.3.1, path loss effect is introduced due to the long-distance signal propagation between mobile users and base stations. On the contrast, small scale fading normally happens in a diminutive scale – the power of received signal varies rapidly and significantly in a small spatial range. Analogous to path loss effect, small scale fading is also determined by the environment travelled by signals. The transmitted signal will be reflected, diffracted and scattered into multipath components in the real world environment [3]. After experiencing reflection, diffraction and scattering, different multipath components would have various amplitude attenuation, time delay and phase changes. As a result, receivers will obtain a constructive or destructive superposition of multipath components. Assume the standard received signal power after path loss effect is  $P_{PL}$ . Then a constructive summation happens when received multipath components have similar phase and time delay, thus the summation signal is enhanced, e.g., higher received power than  $P_{PL}$ . A destructive summation happens when the phase of received multipath components varies a lot, thus the summation signal is depressed, e.g., lower received power than  $P_{PL}$ . When the destruction is very strong then deep fade would occur, and the communication would be blocked due to the poor signal quality.

Several fading models are proposed to simulate the real world fading effects, and Rayleigh fading is the prevalent one that is frequently utilized by researchers. Within this thesis, it is assumed that all transmitted signals between base stations and mobile users experience Rayleigh fading with mean value 1. As discussed in Section 2.3.1, all transmitters apply the transmit power 1 Watt, consequently, the received signal power of a mobile user can be defined by following formula, when the transmitted signal experiences both path loss effect and fading:

$$P_r = \frac{hG_tG_r\lambda_c^2}{(4\pi)^2(d)^\alpha} \quad (2.4)$$

Where  $h$  follows an exponential distribution with mean 1 and  $d$  is the distance between a base station and a mobile user.  $\alpha$  is the path loss factor discussed in Section 2.3.1. As antenna gains and carrier wavelength are constant and pre-determined. Hence, for simplicity, the constant term  $\frac{G_tG_r\lambda_c^2}{4\pi^2}$  is set to have the value 1. Finally, the received signal power of a receiver can be represented as follow:

$$P_r = \frac{h}{(d)^\alpha} \quad (2.5)$$

### 2.3.3 Additive White Gaussian Noise

Within a cellular network, noise may come from internal electronic elements or outside environment. For simplicity, only Additive White Gaussian Noise (AWGN) is considered in the analysis. The AWGN power is represented by  $P_n$ , as a result, the signal-to-noise-ratio (SNR) of a received signal can be defined as follows:

$$SNR = \frac{P_r}{P_n} \quad (2.6)$$

In addition, for a mobile user in downlink access scenario or a base station in uplink access scenario, the total interference power  $P_I$  come from other base stations or mobile users can be calculated as follows:

$$P_I = \sum_{i=1}^{i=N} \frac{h_i}{(d_i)^\alpha} \quad (2.7)$$

Within in this equation,  $N$  stands for the number of the interference sources.  $h_i$  is related to  $h$  in equation 2.4.  $d_i$  represents the distance between the particular receiver and the interference source. Finally, for a mobile user in the downlink access scenario or a base station in uplink access scenario, the signal-to-interference-plus-noise-ratio (SINR) is defined as follows:

$$SINR = \frac{P_r}{P_I + P_n} \quad (2.8)$$

The SINR is one of the most critical performance metrics of a cellular network. Comparing equation 2.6 with 2.8, it can be noticed that 2.8 returns back to 2.6 when the interference is not taken into consideration. Given a SINR threshold, the coverage probability of a cellular network can be calculated because when the SINR is lower than a particular value, the communication between mobile users and base stations would be blocked. In addition, researchers can determine the average achievable rate of the cellular network base on the value of SINR.

## 2.4 Fractional Power Control

This section is dedicated to provide a basic illustration of the power control framework implemented in the uplink access simulation models within this thesis. The power control technique is widely applied to better manage the interferences of a cellular network, and there are numerous proposed power control frameworks in both LTE and CDMA networks [19][20]. Besides, the power control technique also helps

with energy management. For modern cellular network users, battery life is a very important factor that affects mobile user experience since mobile devices normally have limited power [21]. The fractional power control framework is applied in the uplink simulation models within this thesis. Following Figure 2.1 [11] displays an uplink access scenario in a cellular network. For simplicity, the cell boundaries are drawn in oval.

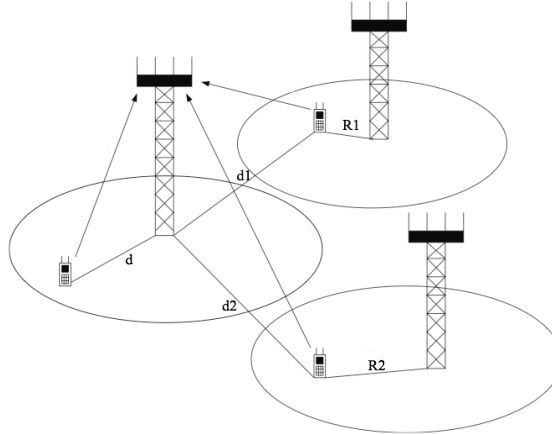


Figure 2.1: Uplink fractional power control model

Figure 2.1 displays the uplink access scenario, within which the mobile users are transmitting data to base stations. Within this figure, the leftmost cellphone is treated as the research target, and it is communicating with the leftmost also the nearest base station, namely, the tagged base station. The tagged distance is  $d$ . The remaining two cellphones are acting as interference sources and the interference distance is  $d_1$  and  $d_2$  respectively. Each interfering cellphone also has its own tagged distance, which is  $R_1$  and  $R_2$  respectively. Wireless fading channel effect can be represented by  $h$ , which is an exponential distribution random variable with mean value 1, and  $P_n$  stands for the AWGN power.  $\alpha$  is the path loss factor while  $\varepsilon$  is the fractional power control factor, varying from 0 to 1, decided by the cellular network settings. Then the SINR at the target mobile user can be written as follows:

$$SINR = \frac{hd^{\alpha(\varepsilon-1)}}{\sum_{i=1}^{i=2} h_i R_i^{\alpha\varepsilon} d_i^{-\alpha} + P_n} \quad (2.9)$$

From the formula, it can be observed that the path loss effect is partially reversed by adding the power control factor.  $hd^{\alpha(\varepsilon-1)}$  in the numerator can be transformed into  $h/d^{\alpha(1-\varepsilon)}$ , showing that when  $\varepsilon$  equals to 1 then the path loss effect is entirely reduced then the received signal power is determined by  $h$ , which is an exponentially distributed random variable with mean value of 1. This analysis means that when a mobile user is closely located to its tagged base station, due to the relatively weak

path loss effect, the mobile user does not have to spend a lot of energy to transmit signals but can still keep acceptable SINR. When the mobile user resides on the cell edge, this mobile user can spend much energy to reverse the path loss effect hence can achieve acceptable SINR. Overall, the fractional power control is a useful tool and is widely applied in communication systems hence it is involved in the uplink access simulation models.

## 2.5 Default Network Settings

Following table displays some default cellular network settings and parameters in all simulation models. In upcoming chapters, unless otherwise indicated, following settings will apply.

Land area ( $m^2$ )	$10^6$
Number of base stations	36
Number of mobile users	1000
Transmission power ( $W$ )	1
AWGN power ( $dBm$ )	-100
Fading model	Rayleigh fading
Path loss factor	4

Table 2.1: Default cellular network settings

## 2.6 Summary

This chapter concentrates on demonstrating the methodologies of constructing the simulation models of cellular network within the research project. In particular, base station deployment methodologies and wireless communication channel model are introduced in detail, as they significantly impact cellular network performance. In addition, basic knowledge of fractional power control is illustrated, and the expression of the received signal power at a target receiver when considering power control is derived. Finally, some default parameters value and networks configurations are displayed. Readers now have obtained knowledge of the basic simulation model, thus future advanced models could be easily accepted.

# Coverage Probability Analysis

---

Coverage probability is one of the most important metrics that is widely utilized to evaluate cellular network performance by researchers. This chapter aims to evaluate the three different cellular network models against the coverage probability metric, in both downlink access scenario and uplink access scenario. Analysis of the cellular network models implementing default network parameters and settings will be carried out firstly. After that, some network parameters such as path loss factor and AWGN power will be treated as variables, to help with providing insight analysis of performance discrepancies between different cellular network models.

Section 3.1 aims to provide the mathematical definition of coverage probability in the cellular network context, and introduce the methodology of calculating coverage probability within this thesis. After that, Section 3.2 and 3.3 particularly demonstrates the coverage probability analysis in the downlink access scenario and uplink access scenario respectively, showing the performance discrepancies among all the three cellular network models. Finally, Section 3.5 serves to summarize the coverage probability analysis chapter.

## 3.1 Coverage Probability Definition

Coverage probability has different definitions in various disciplines. Within the cellular network context, coverage probability represents the likelihood of one signal receiver who can successfully communicate with its tagged transmitter. As discussed in preceding chapters, signal quality, which is mainly represented by SINR, determines whether or not communications can be successfully carried out. If the SINR of a received signal is lower than a particular threshold  $T$ , then the communication will be blocked. Based on this, the coverage probability can be defined as follows:

$$p_c = \mathbb{P}[SINR > T] \quad (3.1)$$

Where  $p_c$  stands for the coverage probability and  $T$  stands for the SINR threshold, which is the minimum required SINR value to achieve successful communications between transmitters and receivers. Apparently the coverage probability can also be calculated as follows:

$$p_c = \frac{N_{SINR>T}}{N} \quad (3.2)$$

Where  $N_{SINR>T}$  stands for the number of signal receivers whose SINR is higher than the threshold while  $N$  stands for the total number of receivers within the entire cellular network. It should be indicated that formula 3.2 is only valid when  $N$  goes to infinite. However, because the simulations procedures in this research project are repeated for many times thus the  $N$  will be a extremely large number, as a result, the outcome of formula 3.2 is relatively accurate. In the following sections of the thesis, unless otherwise indicated, the coverage probability of cellular network models will be calculated by using formula 3.2.

## 3.2 Downlink Access Analysis

Within the downlink access scenario, base stations transmit signals through the wireless channel to mobile users. Mobile users only act as signal receivers and there is no communication between different mobile users as well as different base stations. Within this section, it is presumed that a particular user is communicating with its nearest base station, namely the tagged base station. Also, as introduced in Chapter 1, the frequency spectrum is reused in every cell within all the cellular network models, which means that for every mobile user, interferences come from all base stations except for the tagged base station.

Based on the default cellular network configurations and parameters proposed in Chapter 2, three simulative cellular network models are constructed and displayed in Figure 3.1, Figure 3.2 and Figure 3.3 respectively on next page. Red points stand for the cellular network base stations while green points represent the randomly scattered mobile users in the entire networks. As a result, the distance between a mobile user and a base station can be calculated based on points' spatial coordinates, after that, the received signal power for a particular mobile user can be calculated by using formula 2.5.

This section aims to detailedly demonstrate the analysis of the coverage probability performance discrepancies between the three cellular network models in the

downlink access scenario. Firstly, the coverage probability of the cellular network models with default parameters and settings will be simulated and comparisons will be made. After that, cellular network parameters and configurations such as path loss factor and base station density will be treated as variables in simulation, which can help in better demonstrating coverage probability performance differences among all the three cellular network models.

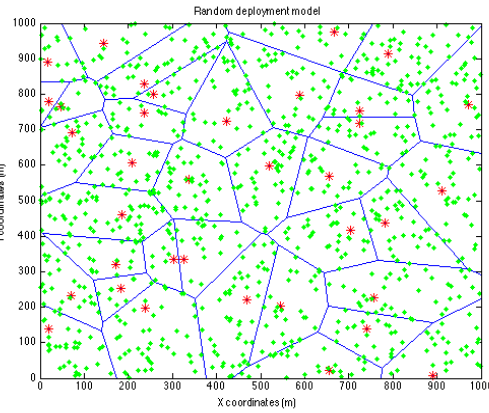


Figure 3.1: Default PPP model

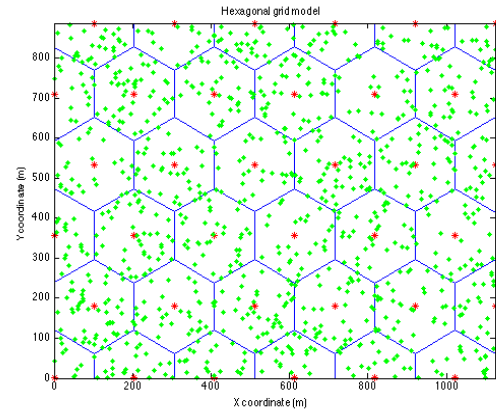


Figure 3.2: Default hexagonal model

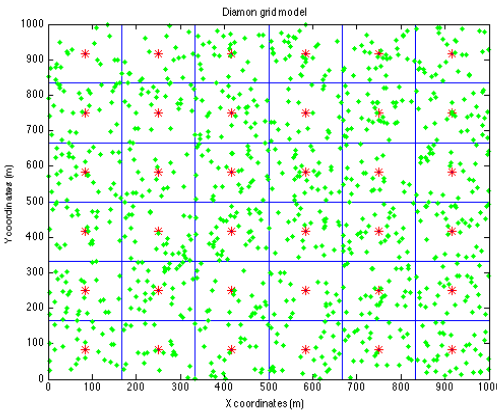


Figure 3.3: Default diamond model

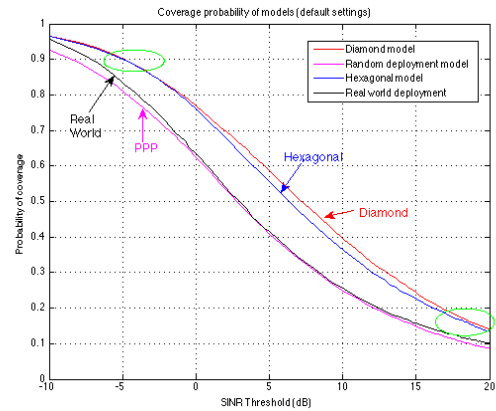


Figure 3.4: Default coverage probabilities

### 3.2.1 Network Models with Default Settings

In Figure 3.4, one train of increasing SINR thresholds in log-scale is set on the x-axis while the coverage probability value is represented by the y-axis. The coverage probability for each cellular network model is calculated by using formula 3.2, which is the average fraction of all mobile users who obtain signal SINR that is greater than the corresponding threshold. In addition, the coverage probability performance of a real world cellular network deployment provided in [7] is also included, to better demonstrate the coverage probability performance discrepancies between simulative

cellular network models and real world cellular networks. However, it should be indicated that the base station locations of the real world deployment within this thesis are obtained by manually measuring the deployment figure given in [7], as a result, errors are existing. In addition, compared with the real world deployment in given in [6], this real world deployment has very random deployment, hence it is inferred that the cellular network performance of this real world deployment will possibly close to the random deployment model. Besides, the real world deployment has base station density  $3.156 \times 10^{-5}/m^2$  as shown in [7], which is smaller than the default base station density  $3.600 \times 10^{-5}/m^2$ . This base station density imperfection will generate inaccuracy of the simulation results, and will be discussed in following contents of the thesis. The rest cellular network settings and parameters are the same in both constructed simulation models and real world deployment.

It can be observed from Figure 3.4 that the random deployment model (PPP line in Figure 3.4) gives the lower bound of coverage probability performance among all the cellular network models in the downlink access scenario. This pessimistic coverage probability of mobile users is caused by the strong interferences generated by other base stations. The origin of the strong interference is that in the random deployment model, base stations will in some case closely locate together but still have a significant coverage area [6], as a result, the distance between a mobile user and its tagged base station will not be significantly larger than other interfering distance, hence the SINR of the received signal will be relatively small, contributing to the low coverage probability performance.

Although the random deployment model provides the lower bound of performance, however, it can be observed that the performance of the random deployment is very close to the real world deployment, which means that the random deployment model is very accurate. The reason is that the real world base station deployment provided in [7] has very random shaped cells, as displayed in Figure 1.4, and this may result from the geometric properties of the land area covered by the cellular network. Other real world cellular networks such as the real world deployment proposed in [6] may have more regular shaped cells. Hence, better coverage probability performance is expected.

Being opposite to the random deployment model, traditional grid models perform much better, as shown in Figure 3.4. The diamond grid model provides the upper bound of coverage probability among all the three cellular network models. However, it can be observed that the coverage probability discrepancies between the diamond grid model and the hexagonal grid model are subtle, especially in low and high SINR

threshold region as shown in the green circles. The maximum performance gap in medium SINR threshold region is still relatively small as well, which is around -17dB.

The coverage probability performance of the real world deployment locates between the upper bound and lower bound. This phenomenon meets the expected result, as the cell shape of the grid models are over ideal, hence the performance is optimal while random deployment model gives lower bound value due to the randomly shaped cell which results in strong interferences. However, it can be observed that the performance discrepancies are small, especially in medium SINR threshold region.

It should be noticed that although the random deployment model gives the lower bound of coverage probability performance, it does not necessarily mean that the random deployment model is not a suitable model for simulating cellular networks. There are two main reasons. The first reason is that the grid models such as diamond grid model have over-ideal cell shape. Hence the coverage probability performance simulation gives optimal values compared with real world performance. On the contrary, the random deployment model gives the lower bound of the coverage probability. This conservative result is more pragmatic than optimal results when analysing the minimum coverage probability and minimum average achievable rate of a real world cellular network. The other reason is that the random deployment model is not only more tractable in mathematical analysis but also relatively accurate, as shown in Figure 3.4, the PPP line shares same trend with the real world deployment line and the two lines of the grid models, and it becomes more precise in medium and high SINR region. Overall, the random deployment model is a useful tool for simulating cellular networks coverage probability performance in the down-link access scenario, according to its high-attractable property and accuracy.

### 3.2.2 Network Models with Various Path Loss Factor

Discussions in Section 3.2.1 focus on the three cellular network models with default network configurations and parameters. However, it is necessary to treat some cellular network parameters such as path loss factor as variables, because the wireless channel properties may vary frequently and significantly due to the complex environment where the transmitted signals travel through.

To begin with, the path loss factor  $\alpha$  will be treated as a variable and has value 2.5, 4.5, 5.5 and 6 respectively while other network settings and parameters remain the same to the default settings. It is expected that changing the path loss factor

would result in apparent alterations in the coverage probability performance. The reason is that according to formula 2.5, the path loss factor is strongly related to the received signal power, which would impact the SINR significantly. The simulation results are displayed in the following figures:

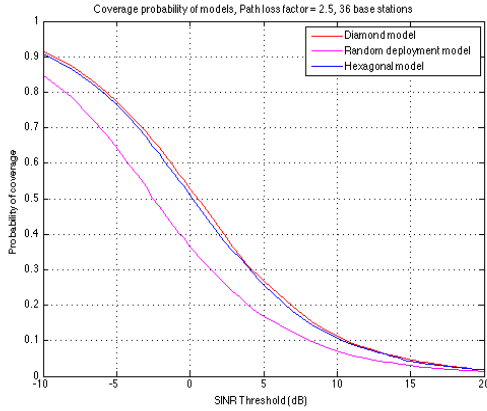


Figure 3.5: Path loss factor is 2.5

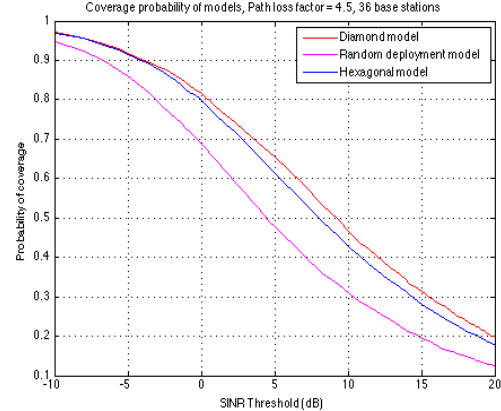


Figure 3.6: Path loss factor is 4.5

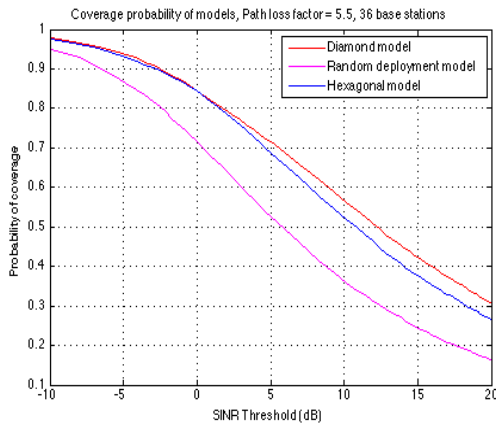


Figure 3.7: Path loss factor is 5.5

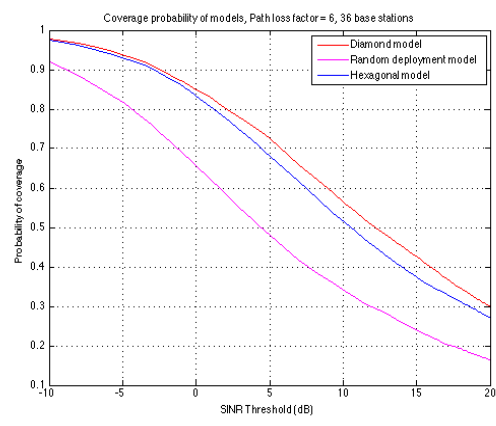


Figure 3.8: Path loss factor is 6

Figure 3.5, 3.6, 3.7 and 3.8 displays the coverage probability performance of all the three cellular network models in the downlink access scenario when the path loss factor  $\alpha$  equals to 2.5, 4.5, 5.5 and 6 respectively. It can be clearly observed from these figures that with the decreasing of path loss factor, the coverage probability performance gap of random deployment model and grid models reduces accordingly, which means that the random deployment model is more accurate when the path factor is relatively small. This phenomenon can be theoretically analysed as follows. As discussed in Chapter 1, because the base station locations in a random deployment model are generated by applying a PPP, hence it is possible for some base stations closely locate to each other but still cover large areas. In this scenario,

those base stations will generate plenty of interferences to a mobile user resides in one cell, and these interferences mainly contribute to the signal SINR calculation. However, this scenario never happens in grid models as the base stations have to reside in the center of each cell. When the path loss factor is relatively small, for a mobile user, interferences from further base stations become larger, because according to formula 2.3, smaller path loss factor means that the energy dissipation effect becomes weaker. As a result, the received interfering signal energy is increased such that the received signal SINR is reduced, result in lower coverage probability as displayed in Figure 3.5. This explains why the coverage probability performance of grid models decreases along with the reduction of path loss factor, and why the random deployment model is more accurate when the path loss factor is relatively small. And when the path loss factor is very large, according to 2.3, the interfering signal power is significantly reduced. As a result, the power of AWGN mainly contributes to the SINR calculation.

It can also be observed that the performance differences between diamond model and hexagonal model are still small in all figures, compared with the performance discrepancies between the random deployment model and both two grid models. Interestingly, it can be discovered that when the path loss factor equals to 2.5, the coverage performances of diamond grid model and hexagonal grid model are nearly the same. However, observing all the above four figures plus Figure 3.4, it can be discovered that the performance gap between the two grid models increases with the growth of path loss factor.

### 3.2.3 Network Models with Various AWGN Power

As introduced in Chapter 2, the default power of AWGN  $P_n$  within the simulation models is  $-100dBm$  in log-scale and  $10^{-13}$  Watts in linear scale. All preceding simulation models apply the default power value, however,  $P_n$  will be treated as a variable in this section to better demonstrate how the power of AWGN impacts the cellular network coverage probability.

Based on formula 2.8, it can be directly inferred that increasing  $P_n$  means increasing the denominator of the equation, then the received signal SINR will decrease accordingly. As a result, the coverage probability performance of cellular networks models will be reduced. The inference is really intuitive and straightforward, and following figures are applied to prove the deduction:

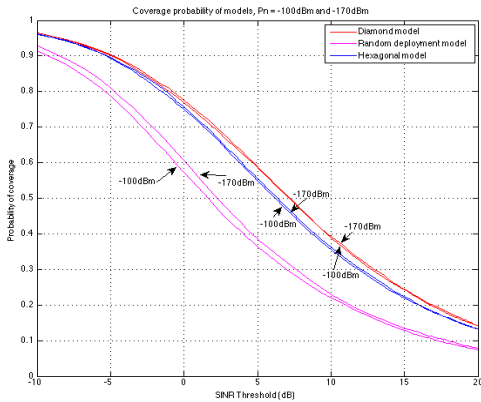
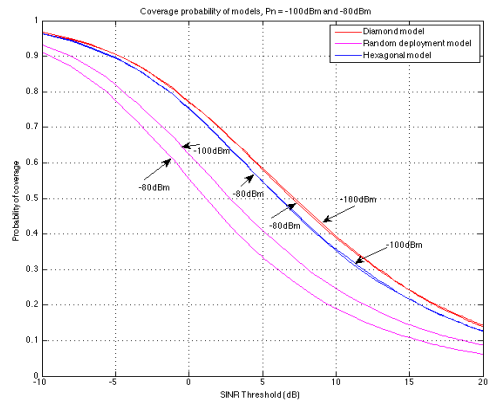
Figure 3.9:  $P_n = -100\text{dBm}$  and  $-170\text{dBm}$ Figure 3.10:  $P_n = -100\text{dBm}$  and  $-80\text{dBm}$ 

Figure 3.9 displays the coverage probability performance differences of all the three cellular network models when the AWGN power is reduced from  $-100\text{dBm}$  to  $-170\text{dBm}$ . As can be observed from Figure 3.9, when the noise power is reduced significantly, the coverage probability performance alterations of the diamond model and hexagonal model are tiny and can be safely ignored. However, the coverage probability alteration of the random deployment model is more evident, compared with that of the grid models. Figure 3.10 illustrates the same trend when the AWGN power is enhanced from  $-100\text{dBm}$  to  $-80\text{dBm}$ . The coverage probability performance of all models are decreased, but the changes between grid models are still small and can be safely neglected while the performance gap between the random deployment model is relatively apparent.

Comparing the performance gaps of grid models and random deployment model, it can be observed that the random deployment model is more sensitive to AWGN power alterations. It can also be discovered that for the random deployment model, the coverage probability performance change is roughly remaining a constant among the entire SINR threshold region, which means that AWGN power changes are not dominating the coverage probability performance in the random deployment model. As a result, unless otherwise indicated, default value of  $P_n$  will be applied consistently in following contents for succinctness.

### 3.2.4 Network Models with Various Base Station Density

Chapter 1 has introduced that in the real world situation, a cellular network covers a large land area and base stations are distributed according to the geometric properties and the population distribution of the land area. An urban area such as a big city has a large population thus requires a lot of base stations to serve mobile users

that are randomly distributed in the area. On the contrary, dense base stations may not be required in rural areas due to the relatively small population and the small amount of mobile users there. In the downlink access scenario, the coverage probability performances of cellular networks models with various base station densities are not identical, as a result, simulations will be carried out to evaluate the coverage probability performance discrepancies within different cellular network models that have various base station densities. Some simulation results are presented by following figures. Default network parameters are applied except for the base station density. In addition, as analysed in above sections and figures, the coverage probability performance of the hexagonal model is very close to that of the diamond grid model. As a result, within this section, the simulation results of hexagonal grid model are omitted.

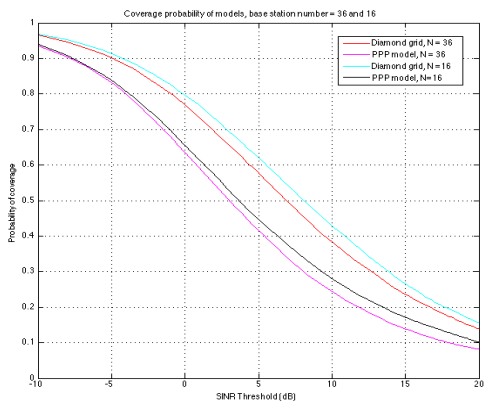


Figure 3.11: 16 and 36 base stations

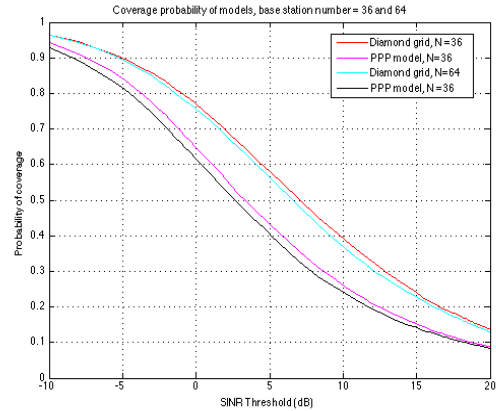


Figure 3.12: 64 and 36 base stations

Figure 3.11 illustrates when the number of base stations in the proposed  $10^6 m^2$  area decreases from 36 to 16, the coverage probability performance alteration of the diamond grid model and the random deployment model. As can be observed, both diamond grid model and random deployment model perform slightly better when the number of base station in the area is reduced. This is intuitive because for a particular mobile user, interferences come from all base stations except for the tagged one and reducing the number of base stations means lessen the number of interfering base stations, resulting in better coverage probability performance. On the contrary, increasing the number of base stations in the proposed area contributes to increasing the number of interfering base stations, result in worse coverage probability performance, as shown in Figure 3.12.

From above two figures, it can be noticed that slightly changing the base station density will not result in apparent coverage probability performance alterations. The

reason is that in the proposed area, fewer interfering base stations also lead to smaller interfering distance while more interfering base stations means larger interfering distance. Due to this trade-off, the base station density will not significantly change the coverage probability performance of the cellular network models, as shown in the small performance alterations in Figure 3.11 and 3.12.

### 3.3 Uplink Access Analysis

Section 3.2 has introduced the coverage probability analysis of the three cellular network models in the downlink access scenario, where mobile users only act as signal receivers and obtain signals from the tagged base station and other interfering base stations. In the uplink access scenario, the roles of base stations and mobile users are interchanged, which means that base stations is going to act as receivers, obtaining transmitted signals from the tagged mobile user and other interfering mobile users. Same to downlink access scenario, frequency spectrum is reused in every cell, which means that for each base station, interferences come from every mobile user that located in other cells.

To carry out the analysis of cellular network models in uplink access scenario, the default network settings and parameters will apply firstly, after that, important parameters will be treated as variables to evaluate the coverage probability performance in uplink access scenario. The default value of AWGN power  $P_n$  is going to be used, and  $P_n$  will not be treated as a variable anymore because it has been proofed that the AWGN power does not dominate the coverage probability performance of the cellular network models. Similar to the AWGN power, the base station density will be treated as a constant as well, which is the default value  $3.600 \times 10^{-5}/m^2$ . However, the fractional power control factor  $\varepsilon$  is going to be taken into consideration and treated as a variable, to demonstrate how the power control technique impacts the coverage probability performance of the three cellular network models in the uplink access scenario.

It should be indicated that the model construction methodology applied to simulate the uplink access scenario is slightly changed to be consistent to the analysis in the downlink access scenario. In Section 3.2, each cell of the three cellular network models encloses a large number of mobile users. However, in the uplink access scenario, although a particular base station still serves a large number of mobile users, but the analysis only focuses on one particular pair of mobile user and base station resided in the cell, which means that in the analysis, there are only one

base station and one mobile user within the cell going to be analysed. The cellular network models structures utilized in the uplink access analysis are displayed in following Figure 3.13, 3.22 and 3.22:

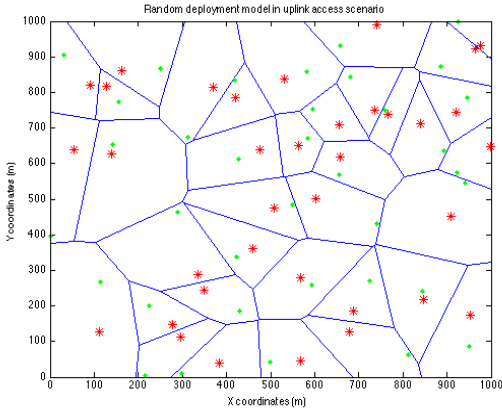


Figure 3.13: Uplink PPP model

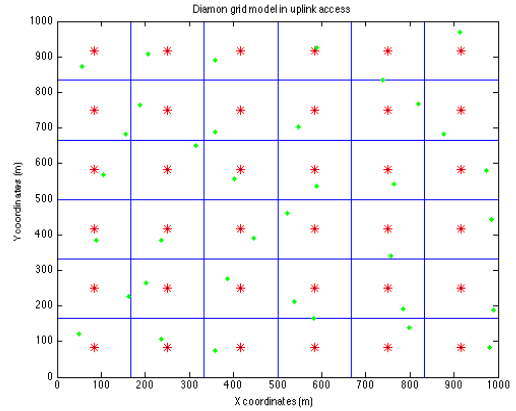


Figure 3.14: Uplink diamond model

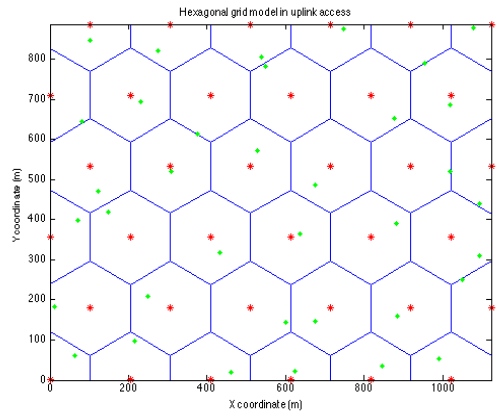


Figure 3.15: Uplink hexagonal model

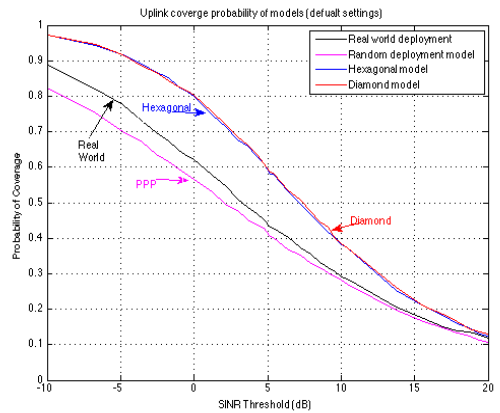


Figure 3.16: Uplink coverage probability

As shown in above figures, red points represent the base station locations while green points stand for the mobile user locations. As introduced above, within each cell, only one mobile user is transmitting the useful signals to the tagged base station while the mobile users located in other cells are sending interfering signals to the base station. In the constructing of uplink access simulation models, guaranteeing only one user locates in each cell is achieved by implementing following steps. To begin with, a large number of mobile users are uniformly scattered in the entire plane. After that, mobile users are removed one by one until each cell only contains one mobile user. Hence within each cell, the mobile user can be considered as uniformly distributed on the cell area. According to this construction process, it can

be discovered that the calculation in the uplink access scenario is more exhausted than that in the downlink access scenario, as a result, the performance lines within the uplink access figures are not as smooth as that in the downlink access performance lines. It can also be noted that analysing the cellular network models in the uplink access scenario is much involved than analysing that in the downlink access scenario. The reason is that according to formula 2.9, for a particular mobile user in the uplink access scenario, the transmitted signal power is depended on the distance between the mobile user and its own tagged base station, due to the implementing of the fractional power control technique. Detailed derivations and mathematical analysis of the distance dependence is proposed in [11]. However, as the core task of this research project is to carry out spatial modelling of different cellular network models, hence the mathematical analysis and derivations relating to the distance dependence is not going to be included.

### 3.3.1 Network Models with Default Settings

Figure 3.16 on previous page illustrates the coverage probability performance of the three cellular network models in the uplink access scenario. Default parameters and network settings are applied, and the fractional power control factor  $\varepsilon$  is assigned with value 0, which means that the power control technique is not considered in generating Figure 3.16. It can be observed that the coverage probability performance of the three network models in uplink access scenario shares the same trend with that in the downlink access scenario. The diamond grid model still provides the upper bound of the coverage probability performance among all the three models while the random deployment model gives the lower bound. In addition, it can be observed that the coverage probability performance gap between the two grid models is minuscule and smaller than that in the downlink access scenario.

Similar to Figure 3.4, the coverage probability performance of the real world base station deployment locates in between the upper bound and lower bound of the performance, which is the expected result. The PPP line in Figure 3.16 strictly follows the trend of the real world deployment, indicating that the random deployment model is still very accurate in simulating the cellular network in uplink access scenario. Considering the mathematical tractable property of the random deployment model, it can be concluded that the random deployment model is also a useful tool that can be applied in researching and analyzing cellular networks in the uplink access scenario.

### 3.3.2 Network Models with Various Path Loss Factor

Figure 3.16 displays the uplink access coverage probability performance of the three proposed network models with default network configurations, which means that the path loss effect factor is 4. Within this section, the path loss factor is going to be treated as a variable to evaluate how the path loss effect impacts the uplink coverage probability performance of the three cellular network models.

Similar to the analysis applied in downlink access scenario, the path loss factor  $\alpha$  is going to be treated as a variable and has value 2.5, 4.5, 5.5 and 6 respectively while the rest network settings and parameters remain the same to the default values. Some simulation results are illustrated by following figures:

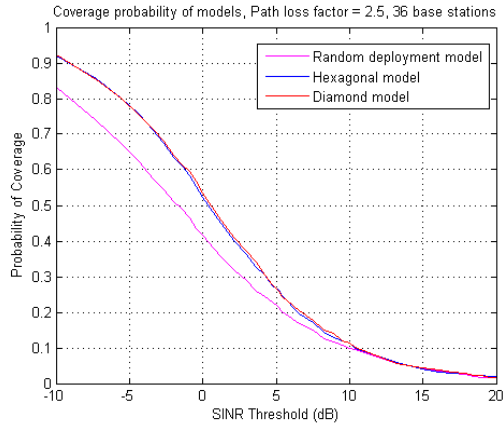


Figure 3.17: Path loss factor is 2.5

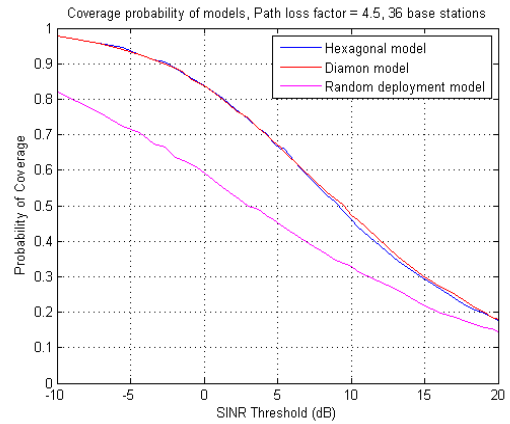


Figure 3.18: Path loss factor is 4.5

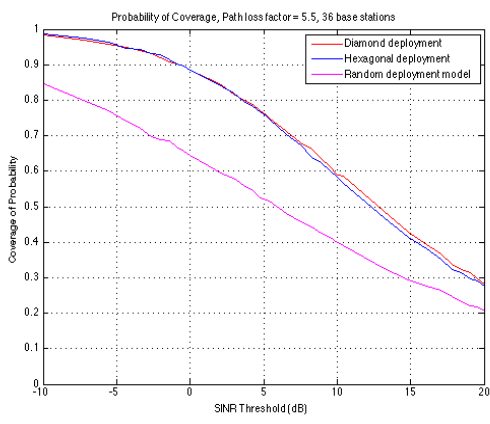


Figure 3.19: Path loss factor is 5.5

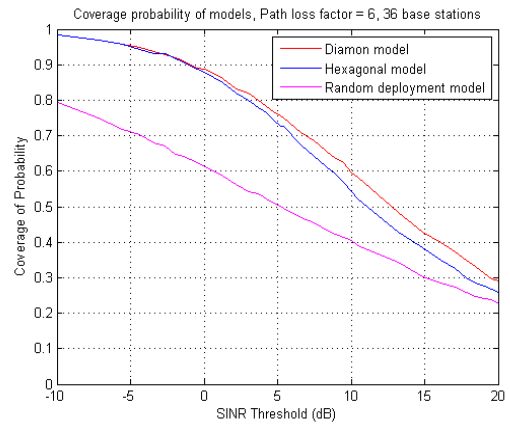


Figure 3.20: Path loss factor is 6

From above four figures, it can be observed that the uplink coverage performance gap between the two grid models is still small, regardless of the variation of the

path loss factor, compared with the performance gap in the downlink access scenario. In addition, observing the above four figures and Figure 3.5, 3.6, 3.7 and 3.8, it can be discovered that the performance gap between the two grid models only becomes distinct in the high SINR threshold region. On the other hand, in the low SINR threshold region, the coverage probability performances of the grid models in both uplink access scenario and downlink access scenario are roughly identical. As a result, it can be inferred that the mathematical expressions for the grid models' coverage probability in both downlink access scenario and uplink access scenario are similar, except for some minor differences. And part of the mathematical analysis and derivations are included in [6].

It can also be observed that although the path loss factor changes from 2.5 to 6, but the coverage probability performance gap between the random deployment model and the grid models in all figures decreases along with the increasing of SINR threshold, which means that within the uplink access scenario, the random deployment model becomes more accurate in the high SINR threshold region.

### 3.3.3 Effects of Changing Power Control Factor

As introduced in Chapter 2, the fractional power control technique is widely applied in the uplink access scenario to better manage the interferences within the cellular network models. It helps to deal with the *near-far* problem where other cell mobile users generate relatively stronger interferences than the transmit power of the tagged mobile user, which frequently happens to the mobile users who locate on the edge of a cell. Besides, it also helps with managing the transmit power of existing electronics mobile devices, which have limited and precious battery life. According to the formula 2.9, it can be mathematically observed that when the power control factor  $\varepsilon$  is assigned with value 1, the path loss effect is totally reversed. However, this does not necessarily mean that  $\varepsilon = 1$  is the optimal choice to obtain good cellular network performance, since the interferences are also increased simultaneously when reversing the path loss effect.

Within the uplink access scenario, choosing the power control factor could be complex. As the mobile users are randomly scattered in the entire plane, there would be some mobile users locate on the edge of a cell while some other mobile users reside in the vicinity of the base stations. Mobile users who locate closely to the base stations may not have to spend a large amount of energy to transmit signals, due to the short distance thus the weak path loss effect. Hence, the best communication strategy for these mobile users would be setting the power control factor  $\varepsilon$  to a

relatively small value to save energy but still can keep acceptable SINR hence good cellular network performance. On the contrary, the mobile users locate on the edge of cells have to spend more energy to reverse the strong path loss effect and overcome the interference from other mobile users. As a result, a larger power control factor  $\varepsilon$  is preferred. Hence, it can be discovered that a trade-off exists when choosing the suitable power control factor. An optimal value of the power control factor which can achieve a overall relatively good cellular network performance is preferred.

In the real world cellular networks, the power control factor is determined by the network properties and configurations to achieve a overall acceptable network performance for most mobile users [22]. As a result, an optimal value of the power control factor will be applied. However, within the uplink access scenario, this optimal value cannot ensure to obtain the optimal network performance over the entire SINR threshold region. Following figures demonstrates the effects of altering the power control factor in different cellular network models:

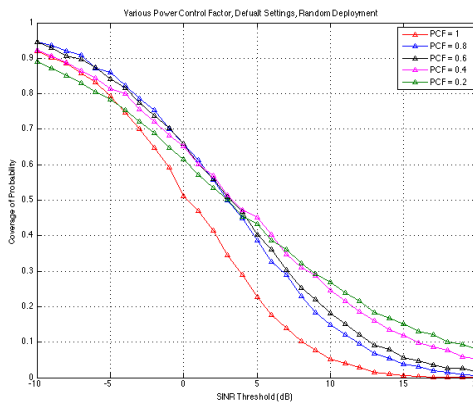


Figure 3.21: PPP model with PCFs

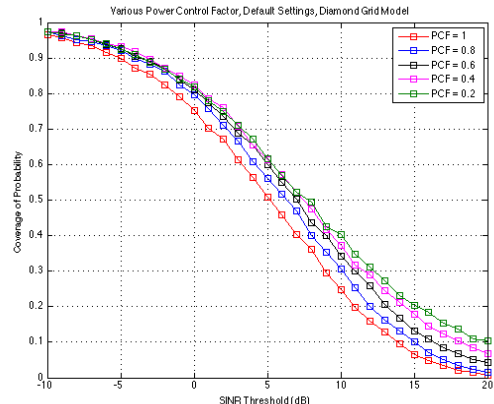


Figure 3.22: Diamond model with PCFs

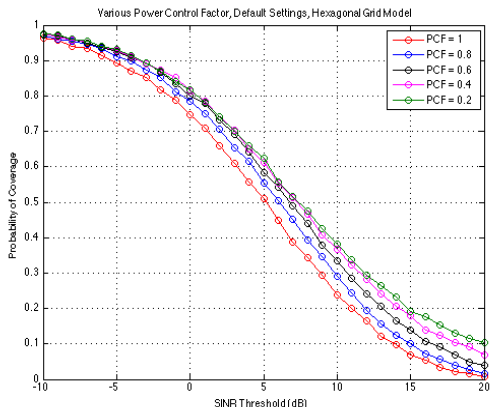


Figure 3.23: Hexagonal model with PCFs

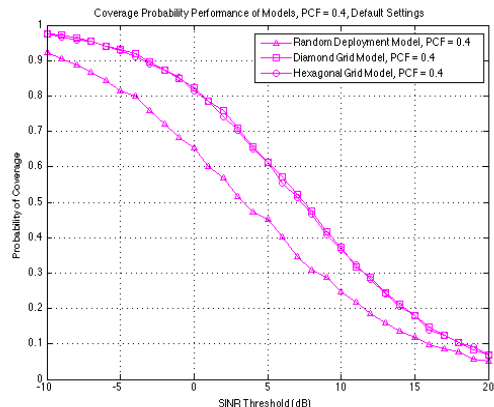


Figure 3.24: Uplink coverage PCF=0.4

Above Figure 3.21, 3.22 and 3.23 displays the uplink coverage probability performance of the random deployment model, diamond grid model and the hexagonal grid model respectively. And the value of the power control factor varies 1 to 0.2. Additionally, Figure 3.24 is dedicated to demonstrate the uplink coverage probability performance discrepancies between the three proposed cellular network models when the power control factor is assigned with value 0.4.

From Figure 3.21, it can be observed that when the SINR threshold is lower than  $5dB$ , the uplink coverage probability performance is optimized when the power control factor has value 0.8. On the other hand,  $\varepsilon = 0.2$  for the random deployment model gives the best uplink coverage probability when the SINR threshold is larger than  $6dB$ . It should be noticed that when the low SINR threshold is smaller than  $5dB$ , the performance discrepancies for  $\varepsilon = 0.8$  and  $\varepsilon = 6$  are tiny hence can be safely neglected.  $\varepsilon = 1$  for the random deployment model gives the worst uplink coverage performance in most SINR threshold region due to the strong interferences generated in entirely compensating the path loss effect of each mobile user.

Figure 3.22 and 3.23 demonstrate how the power control factor can influent the uplink coverage probability performance of the diamond grid model and hexagonal grid model respectively. Comparing these two figures, it can be observed that the uplink coverage probability of these two cellular network models are roughly identical, which means that altering the power control factor will generate same impacts on the performance of these two grid models. From both Figure 3.22 and 3.23, it can be observed that in low SINR threshold region, the performance discrepancies among  $\varepsilon = 0.4$   $\varepsilon = 0.6$  and  $\varepsilon = 0.8$  are tiny, in both diamond grid model and hexagonal grid model. When the SINR threshold increase from around  $5.2dB$  to  $20dB$ , assigning the power control factor with value 0.2 will gives the optimal uplink coverage probability performance. Similar to the random deployment model, when  $\varepsilon = 1$ , grid models also give lowest uplink coverage probability which is the expected result.

Figure 3.24 in previous page demonstrates the uplink coverage probability performance of the three cellular network models when the power control factor is 0.4. The random deployment model gives the lower bound of the coverage performance while the gird models provide the upper bound. This result meets the basic finding of the thesis, and it can be concluded that changing the power control factor will not significantly altering the coverage probability performance distribution of the three cellular network models.

## 3.4 Border Effect

Section 3.2 and 3.3 have demonstrated the coverage probability performance analysis of the three cellular network models in both downlink access scenario and uplink access scenario, and some figures have been displayed to provide pictorial illustrations. However, it should be indicated that when deploying the base stations in all simulative models, the border effect is omitted. The border effect happens in grid models and can be illustrated by using Figure 1.2. Within the downlink access scenario, for a mobile user who resides in the outmost border cells in Figure 1.2, the total received interferences are smaller than that of a mobile user who resides in the central cell, due to the spatial property of the diamond grid model. However, because in the random deployment model, the base stations and mobile users are all randomly scattered in the entire plane, as a result, mobile users in the diamond grid model and hexagonal grid model are also randomly scattered in the whole plane for the consistency of the deployment methodology within this thesis.

To avoid the border effect, some researchers decided to only place mobile users in the central cell, such as the mobile user deployment methodology in [6]. However, comparing the simulation results in [6] and in Section 3.2, it can be seen that the coverage probability performance discrepancy is relatively small. Hence for consistency, the border effect is ignored in this thesis, which means that all mobile users are randomly scattered in the entire plane in every simulative cellular network model.

## 3.5 Summary

Within the coverage probability analysis chapter, the coverage probability of the three cellular network models are studied respectively, in both uplink access and downlink access scenarios. Cellular network models with default parameters and settings are analyzed firstly. Then the path loss factor and other network parameters are treated as variables in analysis.

According to the analysis, it is concluded that the grid models always provide upper bound of the coverage probability performance while the random deployment model gives lower bound. The conservative results provided by the random deployment model are useful in analysing the minimum coverage probability of real world cellular networks. The coverage probability performance gap between the diamond grid model and the hexagonal model are small, hence can be safely ignored. Additionally, based on the analysis, it can be found that the random deployment is also very accurate as it strictly follows the coverage probability performance trend of the real

world deployment and grid models. Considering the accuracy and the conservative results, as well as the mathematical attractive property, it can be concluded that the random deployment model is a useful tool in studying and researching the coverage probability performance of cellular networks.

# Average Achievable Rate Analysis

---

Average achievable rate is another important metric commonly applied in evaluating cellular network performance. With the development of smartphone technologies, the amount of information transmitted between mobile users and base stations is increased significantly. According to Cisco [23], the daily cellular data consumption is about 37.5 megabytes all over the world in April 2015. Hence, analysing the average achievable rate of the three cellular network models is necessary. Unlike Chapter 3, the average achievable rate analysis of this chapter is divided into three major sections, namely downlink access analysis, uplink access analysis and the combined access analysis. Within the combined access scenario, mobile users in a cellular network model are not uniformly utilizing uplink access or downlink access, but have their own access behavior. Within each section, cellular network models with default network settings and configurations will be studied firstly, followed by the analysis of cellular network models that have variable network configurations and parameters.

Section 4.1 serves to demonstrate the mathematical definition and the calculation methodologies of the average achievable rate. Also, a new variable  $K$  is introduced to provide insight analysis of the impacts of same cell user numbers on the average achievable rate performance. Section 4.2 and 4.3 aims to illustrate the analysis of the average achievable rate of the three cellular network models in downlink access scenario and uplink access scenario respectively. Finally, a combined access scenario is introduced to better simulate real world users' behaviors, and the analysis of the combined access scenario will be implemented in Section 4.4. Section 4.5 serves as concluding the whole chapter.

## 4.1 Ergodic Rate and Parameter $K$

### 4.1.1 Ergodic Rate

Nowadays, mobile users can carry out many activities such as website browsing and video streaming by using their smartphones. Although these activities are inter-

esting and various, but the essence of achieving these activities is the information transmitted between smartphones and base stations, through the wired or wireless communication channels. Communication channels have limited ability to transmit information, which is quantified by the *channel capacity*. The definition of the channel capacity comes from the *Shannon–Hartley Theorem* in the information theory, which represents the maximum data rate at which the transmitters and receivers can successfully communicate with each other through a communication channel. The mathematical definition of the channel capacity is illustrated by following formula:

$$C_{cc} = B \times \ln \left( 1 + \frac{S}{P_n} \right) \quad (4.1)$$

Where  $C_{cc}$  stands for the channel capacity,  $B$  represents the channel bandwidth in *Hertz*, which is a constant determined by network settings.  $S$  is the average signal power over the bandwidth in *Watt* while  $P_n$  stands for the AWGN power, which is introduced in Chapter 2. The unit of channel capacity calculated by using formula 4.1 is nats per second, and if the logarithm is taken in base 2, then the unit of  $C_{cc}$  is measured in bits per second. In following analysis, the bandwidth  $B$  will be set to 1 *Hz* for simplicity, and the power of interferences will be taken into consideration since they mainly contribute to the received signal SINR, hence significantly influent the cellular network performance.

After taking the interference into consideration, the average achievable rate, namely the ergodic rate, of the three cellular network models are calculated via averaging the achievable rate of every wireless channel between mobile users and base stations, which means that the methodology of calculating the average achievable rate within this thesis is applying the following formula:

$$C_{nt} = \mathbb{E}[\ln (1 + SINR)] \quad (4.2)$$

Where  $C_{nt}$  stands for the average achievable rate of the cellular network models, and SINR represents the signal-to-interference-plus-noise-ratio of received signal, as introduced in Chapter 2.

#### 4.1.2 Parameter $K$

Within the average achievable rate analysis, the parameter  $K$  is introduced to simulate the average achievable rate performance of the three network models when numerous mobile users are resided in the same cell and share the same frequency

spectrum. For a particular mobile user,  $K$  stands for the number of mobile users who resided in the same cell. Introducing  $K$  means to divide the transmitted signals into different frames, and transmitters are sending the frames successively during their own time slot. This transmit framework is very similar to the Time Division Multiple Access (TDMA), which is a popular access model widely applied in the Global System for Mobile Communications (GSM) system and other 2G cellular systems. After integrating the parameter  $K$ , formula 4.2 can be further written as following formula:

$$C = \mathbb{E} \left[ \frac{1}{K} \times \ln (1 + SINR) \right] \quad (4.3)$$

Where  $C$  is the average achievable rate of a cellular network model.  $K$  represents the number of same cell mobile users for a particular mobile user and has different value for various mobile users who reside in different cells. In following analysis, unless otherwise indicated, the average achievable rate of a cellular network model will be calculated by using formula 4.3.

It can be intuitively noticed that the parameter  $K$  is strongly related to the area of the cell. Because within the proposed cellular network models, the mobile users are scattered on the whole land area according to a PPP, as a result, more mobile users are likely to reside in large area cells instead of the relatively small area cells. Therefore, it can be inferred that within the diamond grid model and the hexagonal grid model, when the total number of mobile users goes to infinite, the parameter  $K$  in different cells is roughly identical and is a constant, and it should be independent with SINR, because the cell area is a constant in grid models.

On the contrary, within the random deployment model, since the base station locations are also generate by using a PPP, as a result, it is possible for some base stations closely locate with each other, hence some of the base stations will cover a small land area, as shown in black rectangles in Figure 1.5. Small area cells are likely to serve less number of mobile users, namely smaller  $K$ . However, for a particular mobile user within the cell, the interference will be relatively large, due to the small distances between the mobile user and interfering base stations, which means the SINR of received signal will be relatively small. Therefore, for the random deployment model, the parameter  $K$  and SINR may not be independent with each other. However, the simulation results in following sections will illustrate that the correlation between the parameter  $K$  and SINR in the random deployment model is not very apparent.

## 4.2 Downlink Access Analysis

This section is dedicated to analyse the average achievable rate performance of the three proposed cellular network models in the downlink access scenario. The detailed illustrations about the downlink access scenario and the pictorial demonstrations of downlink access cellular network structures are demonstrated in Chapter 3. As a result, the introductions about these contents are omitted in this section for concision.

The procedure of analysing the average achievable rate of the three cellular network models in downlink access scenario is similar to the procedures carried out in analysing the downlink coverage probability. To begin with, the average achievable rate analysis of the cellular network models that have default settings and parameters will be carried out. Followed by the analysis of cellular network models that have variable parameters and settings.

### 4.2.1 Network with Default Settings

Within this section, the default cellular network parameters and settings from Table 2.1 are applied to the three cellular network models, except for the AWGN power. According to Table 2.1, the AWGN power  $P_n$  is  $-100dBm$  while the transmit power  $P_t$  of transmitters is  $1Watt$ , as a result, the ratio of the signal transmit power and the AWGN power is  $130dB$ . However, to draw the average achievable rate figures for the cellular network models, this ratio is going to be represented by the x-axis in figures, which means that it will be assigned with different values. Besides, the impacts of introducing the parameter  $K$  in the cellular network models will also be explored. Following figures display the analysis results:

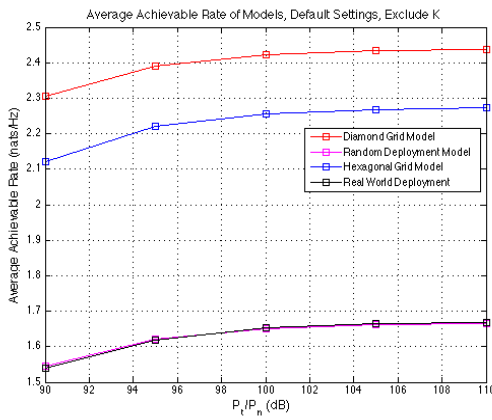


Figure 4.1: Rate of default models (No K)

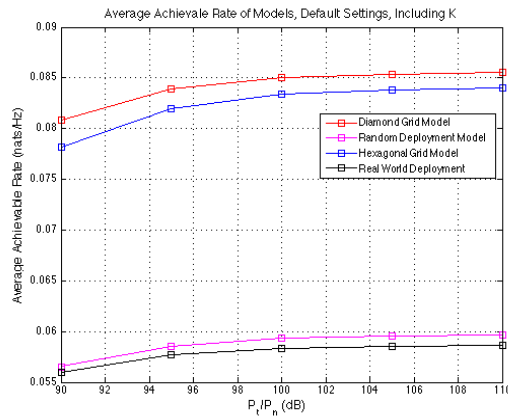


Figure 4.2: Rate of default models

In above two figures, an increasing value sequence from  $90dB$  to  $110dB$  of  $P_t/P_n$  is set on the x-axis while the y-axis represents the average achievable rate of the cellular network models to be evaluated. Additionally, the average achievable rate performance of the real world deployment with default network parameters and settings is also enclosed, as shown by the black lines in above two figures. It should be indicated that to make the comparisons fair, for the real world deployment and the proposed three cellular network models, the same mobile user density is applied, which is  $10^{-3}/m^2$ .

As introduced in Section 4.1.2, the parameter  $K$  stands for the number of mobile users who reside in the same cell of a particular mobile user. Figure 4.1 displays the average achievable rate performance of the cellular network models and the real world deployment, when  $K$  is not taken into consideration. It can be observed from Figure 4.1 that comparing the three cellular network models, the diamond grid model gives the optimal of the average achievable rate performance. The hexagonal grid model provides slightly lower average achievable rate performs than that of the diamond grid model. It can be observed that the rate performance gap between the two grid models is still small, compared with the rate performance gap between the random deployment model and the grid models. Moreover, as can be seen in Figure 4.1 that the real world deployment gives very similar performance of the random deployment model. The reason is that as indicated in Figure 1.4, the real world deployment has very random shaped cells, which is similar to the cells in the random deployment model. As a result, the average achievable rate performance of the real world deployment and the random deployment is quite close, which is similar to the downlink coverage performance. Other real world deployments that have more regular cell shape may perform better.

Figure 4.2 demonstrates the average achievable rate performance of the cellular network deployments when the parameter  $K$  is involved in the analysis. It can be seen from Figure 4.2 that grid models still give the optimal value of the average achievable rate among all the deployments. However, the performance gap between the random deployment model and the real world deployment is slightly enlarged and the rate performance of the random deployment model surpasses the real world deployment. This phenomenon can be analysed as follows. As indicated above, to make fair comparisons, the mobile user density among all models and the real world deployment is identical, which is  $10^{-3}/m^2$ . However, as indicated in Chapter 3, the base station density of the real world deployment is  $3.156 \times 10^{-5}/m^2$ , which is smaller than the default base station density  $3.600 \times 10^{-5}/m^2$ , which is applied in all the three cellular network models. As a result, the average ratio of the number

of mobile users and base stations in the real world deployment is larger than that in the proposed three network models, which means that the base stations in the real world deployment will serve more mobile users than that in the three proposed models, hence when introducing the parameter  $K$ , the real world deployment performs slightly worse than the random deployment model, as shown in Figure 4.2.

To better display the influence of introducing the parameter  $K$  which represents the number of same cell mobile users for a particular mobile user, following tables are constructed when  $P_t/P_n = 90dB$  and  $110dB$ . The numerical data in the following tables is obtained from the generated Figure 4.1 and 4.2 respectively.

**Legend:** *Rate1*: Average achievable rate when  $K$  is excluded in analysis , obtained from Figure 4.1. *Rate2*: Average achievable rate when  $K$  is included in analysis, obtained from Figure 4.2. *MU*: mobile users. *BS*: base stations. #: number

	Rate1	Rate2	Rate1/Rate2	# of MU/# of BS
Diamond grid model	2.3050	0.0821	28.0755	27.7778
Hexagonal grid model	2.1200	0.0782	27.1100	27.7778
Random deployment model	1.5090	0.0565	26.7079	27.7778
Real world deployment	1.5040	0.0560	26.8571	31.6901

Table 4.1: Rate comparison when  $P_t/P_n = 90dB$

	Rate1	Rate2	Rate1/Rate2	# of MU/# of BS
Diamond grid model	2.4070	0.0855	28.1520	27.7778
Hexagonal grid model	2.2730	0.0840	27.0595	27.7778
Random deployment model	1.6260	0.0597	27.2362	27.7778
Real world deployment	1.6360	0.0587	27.8705	31.6901

Table 4.2: Rate comparison when  $P_t/P_n = 110dB$

The data in above Table 4.1 and 4.2 is obtained from Figure 4.1 and 4.2, when  $P_t/P_n = 90dB$  and  $110dB$  respectively. As discussed in preceding Section 4.1.2, because the locations of mobile users are generated according to a PPP, as a result, the number of mobile users who reside in the same cell with a particular cell, namely the parameter  $K$ , is strongly related to the area of this particular cell. Within the two grid models, since cells are identical to each other, as a result, it can be inferred that when the number of mobile users goes to infinite, the parameter  $K$  in the grid models will be constant and can be calculated as the number of mobile users divided

by the number of base stations, which is the fourth column of Table 4.1 and 4.2. As a result, it can be observed that for each grid model, the parameter  $K$ , namely the the number of mobile users divided by the number of base stations, is roughly equal to the average achievable rate ratio, representing that the number of same cell mobile users has simple and intuitive effect on the average achievable rate performance in grid models, which is a simple division algorithm.

Similar to the grid models, for the random deployment model, it can be observed from above two tables that the average achievable rate ratio is also roughly equals to the number of mobiles users divided by the number of base stations, as displayed in the the third column and fourth column of the above tables. This difference is not significant means that the trade-off discussed in Section 4.1.2 is not apparent.

As for the real world deployment, it can be observed that the rate ratio is not strictly equal to the mobile users and base stations ratio. The ratio of  $Rate1$  and  $Rate2$  is smaller than the ratio of the number of mobile users and base station numbers. This is different to the grid models and the random deployment model, where introducing the parameter  $K$  will result in simple division algorithm of the rate performance. Suppose the real world deployment have identical performance of the random deployment model, then the ratio of  $Rate1$  and  $Rate2$  should be roughly 31.6901, which is close to the ratio of mobile users number and base station number. However, it can be observed that the ratio of  $Rate1$  and  $Rate2$  is approximately 27 in reality, which means that introducing the parameter  $K$  will not result in simple division algorithm in the real world deployment. The rate performance reduction is smaller than the ratio of mobile user number and base station number in the real world deployment. This may result from the special trait of the real world deployment. Hence, it is reasonable to infer that when the random deployment model and the real world deployment model have same mobile user density and base station density, the real world deployment analysed in this thesis would perform better than the random deployment model, which means that the random deployment model still possibly gives the lower bound of the average achievable rate performance among the cellular network models. However, it is hard to make general conclusions. More real world deployments are required to propose a general conclusion for the influence of introducing the parameter  $K$ . In the following contents of the thesis, unless otherwise indicated, the parameter  $K$  is consistently applied in all analyses of the three cellular network models.

### 4.2.2 Network with Various Path Loss Factor

This section aims to demonstrate the effects of altering the path loss factor on the average achievable rate performance of the three network models within the downlink access scenario. For simplicity, the path loss factor within this section will be assigned with value 3.5 and 4.5 respectively. The default network settings and parameters are applied except for the variable path loss factor. According to the coverage probability network performance, it is expected that grid models still give optimal rate performance while random deployment model gives lower performance. And the analysis results are illustrated by the following two figures:

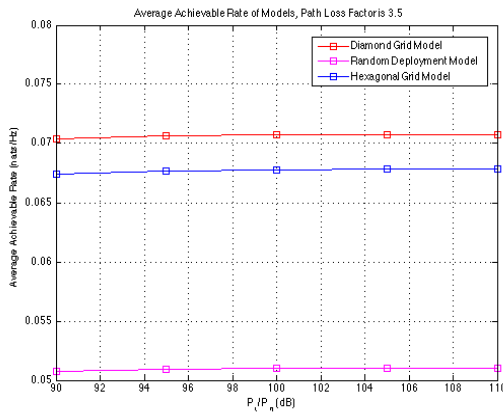


Figure 4.3: Path Loss Factor is 3.5

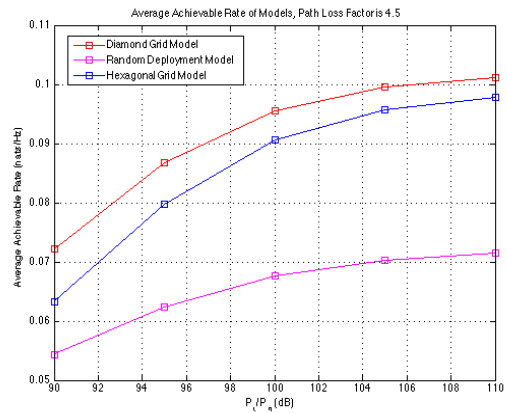


Figure 4.4: Path Loss Factor is 4.5

By observing Figure 4.3 and 4.4, plus Figure 4.2, it can be found that in the downlink access scenario, the random deployment model gives the worst average achievable rate performance among all figures while the diamond grid models gives the optimal rate performance. The average achievable rate performance gap of the diamond grid model and the hexagonal grid model decreases gradually along with the increase of  $P_t/P_n$ , however, this effect is not very apparent. In addition, it can also be discovered that with the increasing of path loss factor, the average achievable rate performance of all the cellular network models changes more obvious along with the increasing  $P_t/P_n$ . When the path loss factor is 3.5, as shown in Figure 4.3, it can be observed that the average achievable rate performance of the three models approximately remain the same when  $P_t/P_n$  varies from 90dB to 110dB. On the contrary, it can be seen from Figure 4.4 that when  $P_t/P_n$  increases from 90dB to 110dB, the average achievable rate performance of the three models gives more obvious alteration when the path loss factor is 4.5. And when the path loss factor is 4, the results in Figure 4.2 give transition between path loss factor is 3.5 and 4.5.

This result can be analysed as follows. According to the path loss effect formula

2.3, when the path loss factor has a relatively small value, the denominator of the formula 2.3 will be smaller than high path loss scenario, as a result, the received power of signals will be relatively high. Under this circumstance, for a particular mobile user, the received power of the interfering signals will have a high value, which means that the interferences power mainly contributes to the calculation of the SINR of the received signals, according to the SINR formula 2.8. As the x-axis in the figures of average achievable rate analysis represents the ratio of transmit power and AWGN power, therefore, the decreasing of the AWGN power will not generate significant alterations of the average achievable rate performance of all the three cellular network models, because the interference power mainly contributes to the calculation of SINR. Therefore, in Figure 4.3, the rate performance lines of the three cellular network models only give small alterations along with the increase of  $P_t/P_n$ .

On the contrary, when the path loss factor is relatively high, namely the path loss effect is very distinct, for a particular mobile user, the total received interferences power will have a relatively low value, due to the strong path loss effect experienced by the interfering signals transmitted by the interfering base stations. As a result, the AWGN power mainly contributes to the calculation of the value of SINR in the high path loss effect scenario, which means that the SINR is more sensitive to the variation of the AWGN power. Therefore, from Figure 4.4, it can be observed that the average achievable rate of the three cellular network models increased apparently along with the increasing of  $P_t/P_n$ .

### 4.3 Uplink Access Analysis

Section 4.2 has introduced the average achievable rate performance of the proposed three cellular network models in the downlink access scenario. Within this section, the uplink access average achievable rate performance of the three cellular network models is going to be evaluated. Similar to the uplink coverage probability performance analysis in Section 3.3, to carry out the analysis of uplink average achievable rate, the default network settings and configurations will be applied firstly. After that, the path loss factor and the uplink power control factor will be treated as variables, and be assigned with different values to evaluate the average achievable rate performance discrepancies between the three cellular network models in the uplink access scenario.

### 4.3.1 Network with Default Settings

Within this section, the analyse procedure is similar to the downlink access scenario. The default network settings and parameters in Table 2.1 is going to be applied to the three cellular network models, except for the various AWGN power. The average achievable rate performance of these three cellular network models with default settings and parameters will be displayed firstly, after that, the effect of introducing the parameter  $K$  in the uplink access scenario will be explored as well, which is similar to the analysis in Section 4.2.1. The simulation results are displayed by the following two figures:

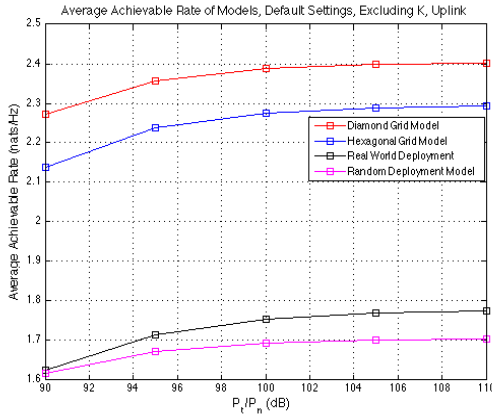


Figure 4.5: Default Uplink Rate (No K)

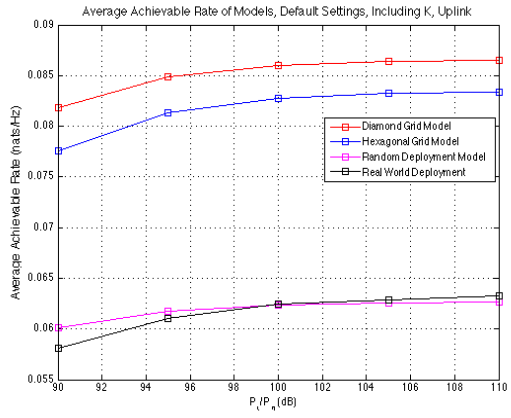


Figure 4.6: Default Uplink Rate

It can be observed from Figure 4.5 that within the uplink access scenario, the random deployment model still provides lower bound of the average achievable rate performance, while the grid models provide the upper bound when the parameter  $K$  is not involved in analysis. By comparing both Figure 4.5 and 4.6, it can be inferred that the parameter  $K$  has the similar impacts on the average achievable rate performance in the uplink access scenario. As a result, the similar procedure in Section 4.2.1 is carried out in this section, to explore the impacts of introducing the parameter  $K$  in the uplink access scenario. According to the numerical data in Figure 4.5 and 4.6, the following tables are constructed:

**Legend:** *Rate1*: Average achievable rate when  $K$  is excluded in analysis , obtained from Figure 4.5. *Rate2*: Average achievable rate when  $K$  is included in analysis, obtained from Figure 4.6. *MU*: mobile users. *BS*: base stations. #: number of

	Rate1	Rate2	Rate1/Rate2	# of MU/# of BS
Diamond grid model	2.2720	0.0818	27.7751	27.7778
Hexagonal grid model	2.1370	0.0776	27.5387	27.7778
Random deployment model	1.6180	0.0601	26.9218	27.7778
Real world deployment	1.6240	0.0581	27.9518	31.6901

Table 4.3: Rate comparison when  $P_t/P_n = 90dB$ 

	Rate1	Rate2	Rate1/Rate2	# of MU/# of BS
Diamond grid model	2.4020	0.0865	27.7688	27.7778
Hexagonal grid model	2.2920	0.0834	27.4820	27.7778
Random deployment model	1.7030	0.0627	27.1611	27.7778
Real world deployment	1.7760	0.0633	28.0569	31.6901

Table 4.4: Rate comparison when  $P_t/P_n = 110dB$ 

According to above Table 4.3 and 4.4, it can be observed that the impacts of introducing the parameter  $K$  in the uplink access scenario is very similar to that in the downlink access scenario. Within the grid models, the average rate ratio is very close to the ratio of number of users and number of base stations. And the random deployment model gives similar results. The real world deployment performs similar to the results in downlink access, and it is reasonable to infer that when the base station density of the real world deployment is equal to the random deployment model, the real world deployment would give better rate performance than the random deployment model. As a result, based on the results in both uplink access analysis and downlink access analysis, it can be concluded that within the proposed three cellular network models in this thesis, introducing the number of same cell mobile users  $K$  will result in approximately  $K$  times decreasing of the average achievable rate performance, and for the random deployment model, the trade-off introduced in Section 4.1.2 is not very apparent, thus can be safely neglected. For real world deployments, the effect of introducing the parameter  $K$  is more complex. To draw general conclusions, more real world deployments should be evaluated.

### 4.3.2 Network with Various Path Loss

This section aims to evaluate the influences of varying the path loss factor on the average achievable rate performance of the three cellular network models in the uplink access scenario. Similar to Section 4.2.2, the path loss factor will also be assigned with 3.5 and 4.5 respectively. It is expected that the average achievable rate performance of the three cellular network models in the uplink access scenario

share the same trend of that in the downlink access scenario. Figure 4.7 and 4.8 as shown below give the simulation results.

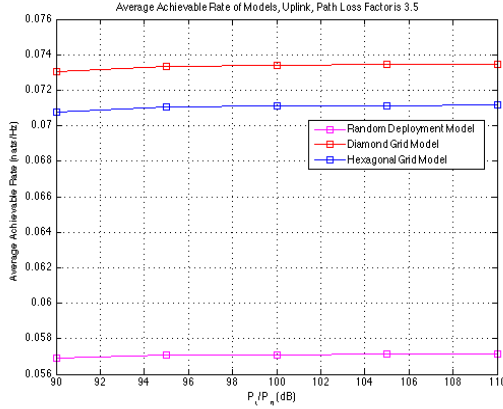


Figure 4.7: Path Loss Factor is 3.5

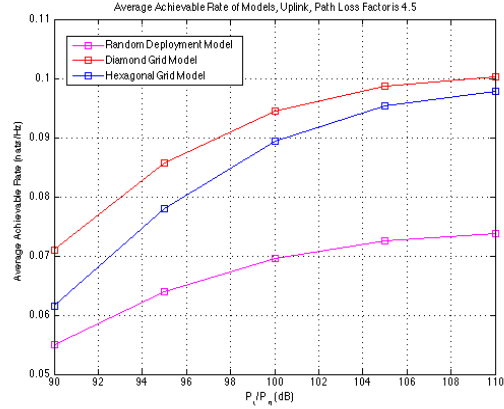


Figure 4.8: Path Loss Factor is 4.5

From the above two figures, it can be observed that the average achievable rate performance of the three cellular network models are also not sensitive to the AWGN power when the path loss factor is relatively small, as the interferences mainly contribute to the calculation of the SINR of the received signals. On the contrary, when the path loss effect is relatively strong, namely larger path loss factor, the rate performance of the cellular network models are sensitive to the AWGN power, result in more significant performance alterations, as shown in Figure 4.8.

By observing the above two figures, it can be concluded that the random deployment model still gives the lower bound of the average achievable rate performance in the uplink access scenario. The grid models share the same rate performance trend with the downlink rate performance, and the performance gap between the two grid models is also not apparent.

### 4.3.3 Network with Various Power Control

As introduced in preceding sections, the power control technique is widely applied in the uplink access scenario, as a result, this section aims to evaluate the impacts of introducing the power control factor in the analysis of average achievable rate analysis. Within this section, the power control factor is assigned with value 1, 0.8, 0.6 and 0.4 respectively. For simplicity, the random deployment model and the diamond grid model are involved in the analysis and following figures demonstrate the average achievable rate differences between the two models:

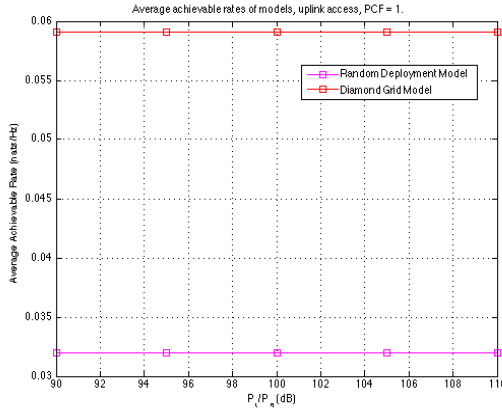


Figure 4.9: Power control factor is 1

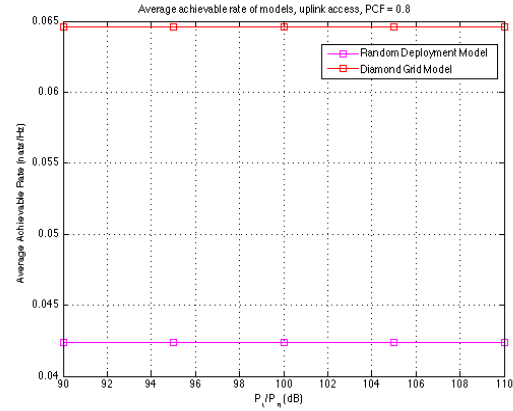


Figure 4.10: Power control factor is 0.8

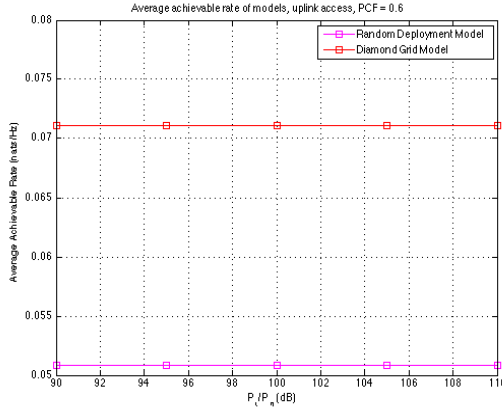


Figure 4.11: Power control factor is 0.6

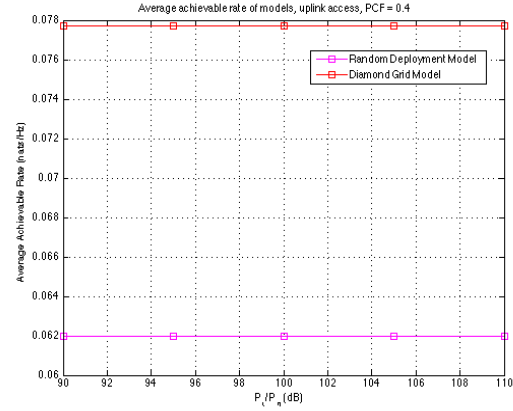


Figure 4.12: Power control factor is 0.4

As can be observed from the above four figures, although the power control factor is changed, but the diamond grid model still provides the upper bound of rate performance and the random deployment model gives the lower bound. When the power control factor is 1, both two models give relatively lower performance, due to the strong interferences generated when the mobile users are trying to totally reverse the path loss effect.

## 4.4 The Combined Access Scenario

Within this section, one combined access scenario is proposed to better simulate the mobile users' behavior in the real world. In the combined access scenario, the mobile users within a cellular network model will not uniformly carry out downlink access or uplink access. On the contrary, each mobile user will decide corresponding access scenarios in the combined access scenario. Within this section, 10000 mobile

users will be scattered in the cellular network models, and the independent variable is the percentage of mobile users who is carrying out the downlink access, where the mobile user act as signal receivers and the base stations act as signal transmitters. There are two dependent variables, which is the average achievable rates of the cellular network models in downlink access scenario and uplink access scenario respectively. Default network settings and parameters except for the number of mobile users are applied in this section, and following figures give the results of the average achievable rate performance of the cellular network models in this combined access scenario:

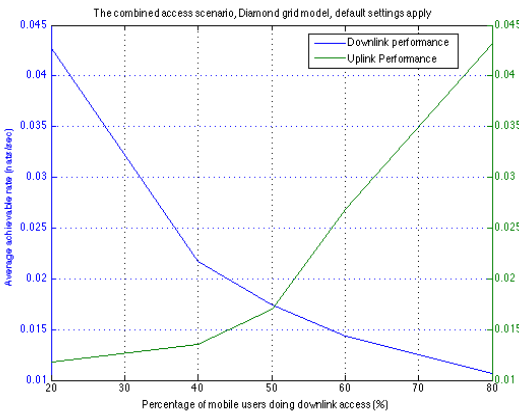


Figure 4.13: Rate of diamond grid model

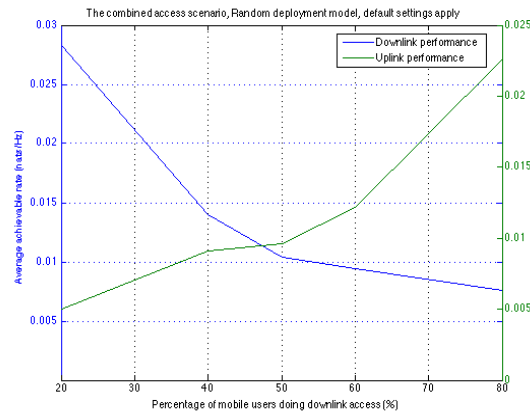


Figure 4.14: Rate of PPP model

Figure 4.13 illustrates the average achievable rate performance of the diamond grid model in the combined access scenario while Figure 4.14 displays the rate performance of the random deployment model. The blue lines and green lines in both two figures represent the downlink access performance and the uplink access performance in the two network models respectively. Observing both two figures, it can be discovered that with the increasing of downlink access users, the downlink access performance in both diamond grid model and the random deployment model decreases gradually. The reason is intuitive, as discussed in preceding sections, the increase of the number of same cell users for a particular mobile user will result in corresponding rate performance reductions. On the contrary, the increasing percentage of mobile users doing downlink access result in the decreasing number of users doing uplink access, as a result, the uplink access performance grows step by step.

It can also be observed that the above two figures are roughly centering symmetric when the half mobile users are utilizing downlink access and another half mobile users doing the uplink access. The reason is that the performance discrepancies

between the downlink access scenario and uplink access scenario are relatively small, as displayed in previous sections. Hence, the above figures are roughly symmetric when equal amount of mobile users are carrying out uplink access and downlink access. Additionally, by carrying out simple calculations, it can be discovered that in the combined access model, the effects of considering the number of same cell users on the downlink access performance and uplink access performance reductions are similar to the effects of introducing the parameter  $K$  in both downlink access scenario and uplink access scenario respectively.

## 4.5 Summary

Within this chapter, the average achievable rate performance of the three cellular network models are analysed, in both uplink access scenario and downlink access scenario respectively. The impacts of introducing the parameter  $K$  is explored. And it is concluded that in the grid models and the random deployment model, introducing  $K$  will result in roughly  $K$  times rate performance reduction, due to the numerous mobile users sharing same spectrum. Although in some figures the real world deployment gives similar or even lower rate performance than the random deployment model when introducing the parameter  $K$  due to the different base station density imperfection, but by analysing the impacts of introducing  $K$  in the real world deployment, it is reasonable to infer that when the base station densities are equal, the real world deployment would give better performance than the random deployment model, which means that the random deployment model still gives the lower bound of the average rate performance. After the analysis of this chapter, it can be observed that the random deployment model still gives the accurate and conservative rate performance, which is similar to the coverage probability analysis. Hence, it is still a useful tool in analysing and studying the cellular networks.

# Conclusion and Future Works

---

## 5.1 Conclusion

This thesis focuses on the spatial modelling and the performance simulation of existing popular cellular network models which are frequently applied in studying the real world cellular networks. Within the thesis, the simulation and the evaluation of the coverage probability performance and the average achievable rate performance of the three cellular network models, namely the diamond grid model, hexagonal grid model and the random deployment model, are carried out in both downlink access scenario and uplink access scenario.

The coverage probability performance analysis is firstly carried out. According to the simulation results, it can be concluded that in both uplink access scenario and downlink access scenario, the random deployment always provide the lower bound of the coverage probability performance. On the contrary, the two grid models always give the upper bound, however, the performance gap between the two grid models is relatively small. Within the average achievable rate analysis, the three proposed cellular models perform similarly to the coverage probability analysis. Grid models perform relatively better than the random deployment model, giving higher average achievable rate in both downlink access scenario and uplink access scenario.

Although the random deployment does not perform well in coverage probability and average achievable rate analysis, but it is still a useful tool to study real world cellular networks. The reason is that in evaluating the real world cellular network performance, the conservative results provided by the random deployment model are more pragmatic than the optimal values provided by the grid models. In addition, researchers have demonstrated that the random deployment model is more mathematically attractable than the grid models, showing that the random deployment model is a helpful tool which can be utilized by researchers to carry out more studies on cellular networks.

## 5.2 Future Works

The thesis allocates emphasis on the spatial modelling of the three cellular network models. As a result, it can be seen that only conceptual analysing is enclosed. Future works may involve quantitative or mathematical analysis, which can accurately explain why the random deployment model gives lower bound of the cellular network performance. Also, the cellular network models applied in the thesis are very preliminary. It is recommended that future works can enclose more advanced wireless communication technologies or more complex network structures in the analysing of the random deployment model, such as MIMO system or heterogeneous networks. More importantly, the base station density discrepancy imperfection between the real world deployment and the three cellular network models results in analysis inaccuracy. Hence, it is strongly recommended that future works should carry out analysis on cellular network deployments that have identical configurations and parameters, which can make sure the analyse results are more precise and reliable.

---

# Bibliography

---

- [1] X. Zhou, *Wireless communications lectures*. The Australian National University, 2014.
- [2] L. O. Walters and P. S. Kritzinger, “Cellular networks: past, present and future,” *Crossroads*, vol. 7, no. 2, pp. 4–ff35, 2000.
- [3] A. Goldsmith, *Wireless communications*. Cambridge University Press, 2005.
- [4] N. Himayat, S. Talwar, A. Rao, and R. Soni, “Interference management for 4g cellular standards [wimax/lte update],” *Communications Magazine, IEEE*, vol. 48, no. 8, pp. 86–92, 2010.
- [5] CISCO, “Global mobile data traffic forecast update, 2014 - 2019,” 2015.
- [6] J. G. Andrews, F. Baccelli, and R. K. Ganti, “A tractable approach to coverage and rate in cellular networks,” *Communications, IEEE Transactions on*, vol. 59, no. 11, pp. 3122–3134, 2011.
- [7] N. Deng, W. Zhou, and M. Haenggi, “The ginibre point process as a model for wireless networks with repulsion,” 2014.
- [8] A. Guidotti, M. Di Renzo, G. E. Corazza, and F. Santucci, “Simplified expression of the average rate of cellular networks using stochastic geometry,” in *Communications (ICC), 2012 IEEE International Conference on*. IEEE, 2012, pp. 2398–2403.
- [9] F. Baccelli, M. Klein, M. Lebourges, and S. Zuyev, “Stochastic geometry and architecture of communication networks,” *Telecommunication Systems*, vol. 7, no. 1-3, pp. 209–227, 1997.
- [10] H. ElSawy and E. Hossain, “Analysis of uplink transmissions in cellular networks: A stochastic geometry approach,” in *Communications (ICC), 2014 IEEE International Conference on*. IEEE, 2014, pp. 5783–5789.
- [11] T. D. Novlan, H. S. Dhillon, and J. G. Andrews, “Analytical modeling of uplink cellular networks,” *Wireless Communications, IEEE Transactions on*, vol. 12, no. 6, pp. 2669–2679, 2013.

- [12] P. Guan and M. Di Renzo, “Stochastic geometry analysis of the average error probability of downlink cellular networks,” in *Computing, Networking and Communications (ICNC), 2014 International Conference on*. IEEE, 2014, pp. 649–655.
- [13] L. Decreusefond, P. Martins, and T.-T. Vu, “An analytical model for evaluating outage and handover probability of cellular wireless networks,” *arXiv preprint arXiv:1009.0193*, 2010.
- [14] X. Ge, B. Yang, J. Ye, G. Mao, C. Wang, and T. Han, “Spatial spectrum and energy efficiency of random cellular networks,” 2015.
- [15] M. Haenggi, *Stochastic geometry for wireless networks*. Cambridge University Press, 2012.
- [16] B. Blaszczyszyn, M. K. Karray, and H. P. Keeler, “Using poisson processes to model lattice cellular networks,” in *INFOCOM, 2013 Proceedings IEEE*. IEEE, 2013, pp. 773–781.
- [17] A. Guo and M. Haenggi, “Spatial stochastic models and metrics for the structure of base stations in cellular networks,” *Wireless Communications, IEEE Transactions on*, vol. 12, no. 11, pp. 5800–5812, 2013.
- [18] M. Pinsky and S. Karlin, *An introduction to stochastic modeling*. Academic Press, 2010.
- [19] C. U. Castellanos, D. L. Villa, C. Rosa, K. I. Pedersen, F. D. Calabrese, P.-H. Michaelsen, and J. Michel, “Performance of uplink fractional power control in utran lte,” in *Vehicular Technology Conference, 2008. VTC Spring 2008. IEEE*. IEEE, 2008, pp. 2517–2521.
- [20] X. Feng, H.-C. Wu, and H. Jiang, “A new approach for optimal power control in the uplink of cellular cdma systems,” in *Communications and Mobile Computing (CMC), 2011 Third International Conference on*. IEEE, 2011, pp. 371–374.
- [21] M. Chiang, P. Hande, T. Lan, and C. W. Tan, “Power control in wireless cellular networks,” *Foundations and Trends® in Networking*, vol. 2, no. 4, pp. 381–533, 2008.
- [22] A. Simonsson and A. Furuskar, “Uplink power control in lte-overview and performance, subtitle: principles and benefits of utilizing rather than compensating for sinr variations,” in *Vehicular Technology Conference, 2008. VTC 2008-Fall. IEEE 68th*. IEEE, 2008, pp. 1–5.

- [23] *Cisco data meter.* The Cisco system, 2015.